

Cross-scale impact of climate temporal variability on ecosystem water and carbon fluxes

Athanasios Paschalis^{a,b*}, Simone Fatichi^b, Gabriel G. Katul^{a,c}, Valeriy Y. Ivanov^d

^a *Nicholas School of the Environment, Duke University*

^b *Institute of Environmental Engineering, ETH Zurich*

^c *Department of Civil and Environmental Engineering, Duke University*

^d *Department of Civil and Environmental Engineering, University of Michigan*

*Corresponding author: athanasios.paschalis@duke.edu

Abstract

While the importance of ecosystem functioning is undisputed in the context of climate change and earth system modeling, the role of short scale temporal variability of hydro-meteorological forcing (~1 hour) on the related ecosystem processes remains to be fully understood. Various impacts of meteorological forcing variability on water and carbon fluxes across a range of scales are explored here using numerical simulations. Synthetic meteorological drivers that highlight dynamic features of the short temporal scale in series of precipitation, temperature, and radiation are constructed. These drivers force a mechanistic ecohydrological model that propagates information content into the dynamics of water and carbon fluxes for an ensemble of representative ecosystems. The focus of the analysis is on a cross-scale effect of the short scale forcing variability on the modeled evapotranspiration and ecosystem carbon assimilation. Interannual variability of water and carbon fluxes is emphasized in the analysis. The main study inferences are summarized as follows: (a) short scale variability of meteorological input does affect water and carbon fluxes across a wide range of time scales, spanning from the hourly to the annual and longer scales; (b) different ecosystems respond to the various characteristics of the short scale variability of the climate forcing in various ways, depending on dominant factors limiting system productivity; (c) whenever short scale variability of meteorological forcing influences primarily fast processes such as photosynthesis, its impact on the slow scale variability of water and carbon fluxes is small; (d) whenever short scale variability of the meteorological forcing impacts slow processes such as movement and storage of water in the soil, the effects of the variability can propagate to annual and longer time scales.

This is the author manuscript accepted for publication and has undergone full peer review but has not been through the copyediting, typesetting, pagination and proofreading process, which may lead to differences between this version and the Version of Record. Please cite this article as doi: [10.1002/2015JG003002](https://doi.org/10.1002/2015JG003002)

August 7, 2015, Manuscript submitted to *Journal of Geophysical Research, Biogeosciences*

32 **Keywords:** *cross-scale interactions, ecohydrological modeling, ecosystem response, interannual*
33 *variability, short scale temporal climate variability, spectral analysis.*

34 **1 Introduction**

35 Climate varies across a wide range of temporal and spatial scales [McManus, 1999] and this
36 variability affects and is affected by vegetation. In particular, the carbon cycle is sensitive to
37 climate variability through multiple processes operating on different time scales such as
38 vegetation growth, mortality and competition [Wilson and Baldocchi, 2000; Bonan, 2008; Sitch
39 *et al.*, 2008; Arora *et al.*, 2013; Friedlingstein *et al.*, 2014]. Considering the rapid change in climate
40 and its variability as projected by the last generation climate models [IPCC, 2013], it is becoming
41 necessary to quantify the associated responses of ecosystems in terms of water and carbon fluxes
42 and their feedbacks to the climate [Medvigy *et al.*, 2010; Reichstein *et al.*, 2013]. The importance
43 of these responses is potentially large, given the potential economic and societal effects resulting
44 from loss of wood yield or food production, and accelerated desertification of semi-arid areas, to
45 name a few.

46 The statistical features of climatic forcing such as air temperature and precipitation evolve in
47 terms of magnitude and variability [Karl *et al.*, 1995; Boer, 2009; Medvigy and Beaulieu, 2012;
48 Sun *et al.*, 2012; Cattiaux *et al.*, 2015]. Changes concerning climate variability include alternation
49 of precipitation and temperature extremes [Allan and Soden, 2008; O’Gorman and Schneider,
50 2009; Kharin *et al.*, 2013], changes in precipitation frequency [Sun *et al.*, 2007] and amounts,
51 changes in the diurnal patterns of temperature and humidity [Vinnikov, 2002; Cattiaux *et al.*,
52 2015; Fatichi *et al.*, 2015], and changes in the variability of the incoming solar radiation
53 [Medvigy and Beaulieu, 2012], among others. In particular, variability at the short temporal scales
54 (e.g. intra-annual to sub-daily) has been found to have a major significance for ecosystems
55 [Medvigy *et al.*, 2010; Fatichi and Ivanov, 2014; Vico *et al.*, 2014]. Variability at such scales is
56 also essential for the hydrological cycle, which in turn influences vegetation in different ways
57 across biomes.

58 The variability of the meteorological forcing can affect ecosystem functions in various ways. For
59 example, precipitation structure determines the root zone soil water availability, which in turn
60 affects plant productivity and thus carbon and water fluxes through photosynthesis and
61 transpiration [Fay *et al.*, 2000; Huxman *et al.*, 2004b]. Temperature variability at small scales
62 (e.g. hours-days), and the temperature correlation structure defining cold or heat wave persistence
63 can affect vegetation productivity and water fluxes (e.g. evapotranspiration) through its impact on

64 the energy balance of the ecosystem, as well as biochemical processes related to carbon fluxes
65 (e.g. photosynthesis and respiration) [Asseng *et al.*, 2011]. Changes in temperature diurnal
66 patterns have been also found to affect vegetation functioning and soil biogeochemistry [Collatz
67 *et al.*, 2000; Peng *et al.*, 2013; Xia *et al.*, 2014]. Radiation variability at the small temporal scales
68 (e.g. hours-days), can also affect the energy balance of the ecosystems, because of the non-
69 linearity embedded in radiation dependent processes.

70 The responses of ecosystems to environmental drivers are generally difficult to quantify due to
71 the large number of nonlinear feedbacks among biological, ecological and hydrological processes
72 occurring at multiple scales [Eagleson, 1978; Laio *et al.*, 2001; Rodriguez-Iturbe *et al.*, 2001;
73 Katul *et al.*, 2007b; Thornton *et al.*, 2014]. Early studies attempted to relate the amount of water
74 and carbon fluxes to mean annual environmental drivers with the goal of extrapolating them to
75 future climates [Fang *et al.*, 2001; Knapp and Smith, 2001; Huxman *et al.*, 2004a]. Arguably the
76 most common relation in hydrology is the Budyko's curve [Donohue *et al.*, 2007; Li *et al.*, 2013]
77 that relates long-term evaporation to dryness indices.

78 It is widely recognized that Budyko's curve or similar empirical relations have predictive skill at
79 the global scale and are able to unfold connections between resource limitations (energy versus
80 water) when discerning some ecosystem responses (e.g. water loss). However, their predictive
81 skill degrades at local scales due to the influence of heterogeneities in forcing and boundary
82 conditions, which affect water and carbon fluxes and storage at smaller spatial and temporal
83 scales [Knapp and Smith, 2001; Stoy *et al.*, 2006; Brooks *et al.*, 2011; Fatichi and Ivanov, 2014;
84 Pappas *et al.*, 2015]. The recognition that short scale climate variability impacts ecosystem
85 functioning [Huxman *et al.*, 2004b; Jentsch *et al.*, 2007; Medvigy *et al.*, 2010] has led to
86 significant advances in eco-hydrology, and motivates this study.

87 To assess the relevance of short scale variability of environmental drivers on carbon-water fluxes
88 and storage, several experimental studies have been conducted. Results from these experiments
89 highlight the significance of short scale temporal variability and statistical structure of
90 precipitation on vegetation dynamics [Swemmer *et al.*, 2007; Heisler-White *et al.*, 2008; Fay *et al.*,
91 2011], and the role of temperature distribution and structure (e.g. diurnal variations) [Wan *et al.*,
92 2002; De Boeck *et al.*, 2010; Wu *et al.*, 2011; Peng *et al.*, 2013; Xia *et al.*, 2014]. Even though
93 experiments provide necessary information about vegetation response to climatic fluctuations,
94 technical and resource limitations typically constrain generality of such experiments. In

95 particular, the complexity of the soil-vegetation-atmosphere system precludes the experimental
96 manipulation of many of the existing feedbacks between biological and hydrological processes.

97 In the last decade, simultaneous advances in understanding ecosystem functioning and the
98 increases in computational capabilities have led to the development of numerical models that
99 resolve the essential hydrological and ecological processes at the relevant scales [Sitch *et al.*,
100 2003; Krinner *et al.*, 2005a; Ivanov *et al.*, 2008; Fatichi *et al.*, 2012b]. These models offer
101 practical tools to construct and test hypotheses about the role of short scale variability in
102 hydrological, ecological and climate studies [Sitch *et al.*, 2008; Gonzalez *et al.*, 2010; Medvigy *et*
103 *al.*, 2010]. A major advantage of using such models is that known feedbacks between soil,
104 vegetation and the atmosphere can be quantified, and thus a generalized assessment concerning
105 the influence of the variability of the environmental drivers on water and carbon fluxes can be
106 outlined.

107 Using one of such mechanistic models, the overarching question we address here is how short
108 scale and inter-annual variability of meteorological forcing affects water and carbon fluxes of
109 various ecosystems spanning a range from boreal forests to semi-arid shrublands. The focus is on
110 precipitation, temperature, and radiation because the responses of ecosystems to these
111 environmental variables are reasonably well understood. Other variables that evolve slowly in
112 time such as the atmospheric CO₂ are not considered. Also, other features of the high frequency
113 variability, such as spring frost damage, known to be impacted by rapid excursions in air
114 temperature variability, are not explicitly considered [Rigby and Porporato, 2008].

115 The elements of hydrometeorologic variability investigated here are: i) The interannual variability
116 of the climate forcing; ii) The auto- and cross- correlation of hourly precipitation, temperature,
117 and radiation; iii) The precipitation structure, and its intermittency patterns (i.e. organization in
118 storm events); and iv) The probability distribution of precipitation, temperature, and radiation,
119 with an emphasis on their extremes. The analysis is based on a comprehensive numerical
120 experimentation with the state-of-the-science T&C ecohydrological model [Fatichi, 2010; Fatichi
121 *et al.*, 2012b], a tool that integrates essential hydrological and plant physiological processes. The
122 effects of temporal variability of climatic forcing on evapotranspiration (*ET*), and its partition
123 into subcomponents, and plant productivity are the main focus. Physical interpretations of the
124 mechanisms that affect *ET* and plant productivity for the analyzed ecosystems across temporal
125 scales are provided. As a practical outcome for planning future field (and numerical) experiments,

126 we seek generalizations that can be used as guidelines for assessing ecosystem responses to a
127 changing climate [Smith *et al.*, 2014; Kayler *et al.*, 2015].

128 **2 Case studies and data**

129 Data from 6 biomes located in 5 different sites are used. The sites investigated are: i) a deciduous
130 forest at the University of Michigan Biological Station (UMBS) in Michigan, USA, ii) a boreal
131 pine forest in the Hyytiälä field station (SMEAR II) in southern Finland, iii) a semiarid shrubland
132 in Lucky Hills, Arizona, USA, iv) a tropical rainforest near Manaus, Brazil, and v) an evergreen
133 pine stand and a deciduous hardwood forest near Durham (Duke Forest), North Carolina, USA. In
134 Figure 1, a brief summary of the sites and their climate is provided (Figure 1b) as well as the
135 simulated annual water use and light use efficiency (Figure 1a). Data from these sites have been
136 extensively analyzed before [Scott *et al.*, 2000; Oren *et al.*, 2001; Yuan *et al.*, 2007; Ivanov *et al.*,
137 2010; Restrepo-Coupe *et al.*, 2013] and only a brief description is provided here.

138 Lucky Hills (110.30W, 31.44N; elevation 1372 m a.s.l.) is located in the Walnut Gulch
139 experimental catchment in Arizona [Keifer *et al.*, 2008; Renard *et al.*, 2008; Paschalis *et al.*,
140 2014b]. Vegetation in this site is sparse and consists of various types of shrubs (deciduous
141 whitethorn acacia and evergreen tarbush, and creosotebush). The soil type is sandy-loam with a
142 relatively low water holding capacity and high permeability [Ritchie *et al.*, 2005]. The assumed
143 soil depth is 2 m and root-zone depth is 0.9 m. Vegetation productivity in Lucky Hills is limited
144 by water availability due to low precipitation and its uneven distribution during the year
145 controlled by the North American Monsoon and also due to a high evaporative demand.
146 Meteorological data for the time period 1996-2009, collected by United States Department of
147 Agriculture- Agricultural Research Service, Southwest Watershed Research Center are used.

148 The deciduous forest in UMBS (84.71W, 45.55N; elevation 234 m a.s.l.) consists primarily of
149 aspen trees, and a smaller fraction of northern red oak, paper birch, American beech, sugar maple,
150 red maple and white pine [Curtis *et al.*, 2005; Gough *et al.*, 2008, 2013; Fatichi and Ivanov,
151 2014]. The soil in the forest is sandy (98% sand), with a low percentage of organic matter and
152 small water holding capacity [Pregitzer *et al.*, 1993]. The assumed soil depth is 3 m and root-
153 zone depth is assumed to be 0.8 m [He *et al.*, 2013]. Plant productivity in UMBS is mostly limited
154 by low temperatures. For this site, 12 years of available data (1999-2010) were used.
155 Meteorological and eddy covariance data were collected at the 33 m tall tower, part of
156 AmeriFlux.

157 The tropical rainforest site (60.21W, 2.61S; elevation 67 m a.s.l.) is located in the Cuieiras
158 reserve near Manaus in Northern Brazil and is part of the Large-Scale Biosphere Atmosphere
159 Experiment in Amazonia (LBA). Vegetation consists primarily of broadleaf evergreen trees
160 [Araújo *et al.*, 2002]. The soil consists of a nutrient poor deep clayey soil. The root system of the
161 trees in the Amazon rain forest is known to be extensive and have access to the deep water
162 storage even during the dry season [Nepstad *et al.*, 1994; Markewitz *et al.*, 2010; Ivanov *et al.*,
163 2012a], potentially enhanced by processes such as hydraulic lift [Oliveira *et al.*, 2005; Yan and
164 Dickinson, 2014]. Meteorological and flux data are collected at a 50 m tall tower (Fluxnet site:
165 Manaus - ZF2 K34) operating since 1999. Vegetation productivity at this site is assumed to be
166 light limited, even though nutrients may play a very important role on this ecosystem [Körner,
167 2009]. In particular, enhanced carbon gain typically occurs during the dry season when light
168 availability is higher and photosynthesis is likely to be more efficient [Saleska *et al.*, 2003, 2007;
169 Hutyra *et al.*, 2007; Myneni *et al.*, 2007; Kim *et al.*, 2012]. However, results that indicate that the
170 rainforest in Manaus may not be particularly limited by radiation, as has been also reported by
171 [Restrepo-Coupe *et al.*, 2013]. In this study, the soil depth was assumed to extend to 14 m and the
172 root depth to 10 m. Meteorological data for the time period 1999-2005 are used.

173 The SMEAR II site (24.17E, 61.51N; elevation 181 m a.s.l.) is located in a Scots pine plantation
174 in southern Finland established in 1962 [Pumpanen *et al.*, 2003; Kolari *et al.*, 2004]. The soil is a
175 low fertility silty sand confined by an impermeable bedrock [Pumpanen *et al.*, 2003; Suni *et al.*,
176 2003]. The soil depth is assumed to extend to 3 m and the root zone to 0.8 m. Hydro-
177 meteorological and flux data for this site were measured at a 73 m tower from 1996 to 2013,
178 operated by the University of Helsinki. The main limitations to photosynthesis are light
179 availability due to the high latitude, low temperature and, occasionally, by low water availability,
180 due to the relatively small precipitation.

181 Finally, two adjacent sites located within the Duke Forest (79.09W, 35.98N, 168 m a.s.l.; pine
182 forest –and hardwood forest) are also explored as these sites represent similar climate and soil
183 type but different vegetation covers. The first is a loblolly pine plantation established in 1983
184 from 3-year old seedlings [Pritchard *et al.*, 2008]. The understory of this loblolly pine forest
185 consists of several deciduous species (red maple, sweetgum, tulip poplar, redbud) that have
186 established since then. The other site is a second-growth 120-year old southern oak-hickory
187 hardwood forest that consists of several unevenly aged deciduous species such as tulip poplar,
188 hickory, various types of oaks (white, chestnut, willow) and sweetgum [Palmroth *et al.*, 2005;
189 Stoy *et al.*, 2007]. The soil type of all sites is a shallow, nutrient poor silt loam with an

190 impermeable clay pan at ~30cm depth [Oishi *et al.*, 2010] that formed due to prior land-use
191 history. Meteorological data were obtained at adjacent flux towers installed at each site as part of
192 the global micrometeorological measurement network Fluxnet [Baldocchi *et al.*, 2001] over the
193 period 1998 – 2008 and operated by Duke University. Vegetation productivity at the Duke forest
194 during the period when leaves are present is not clearly limited by any environmental factor due
195 to above freezing temperatures for most of the year, and high light and water availability. Air
196 temperature and radiation (day-length) are controlling factors of the phenological status of the
197 hardwood forest. Phenology is explicitly resolved in the used model but it is only marginally
198 impacted by high frequency variations, due to the assumed parameterizations.

199 For all the sites used in this study, with the exception of Manaus, gaps in the meteorological data
200 did not exceed 5%. Missing values for all meteorological variables except precipitation were
201 filled with linear interpolation from their neighboring hourly observations, when the gaps were
202 isolated, or given their mean climatological value, preserving the seasonality and the diurnal
203 cycle, in the cases where continuous gaps of data were present. For precipitation, missing values
204 were filled with zeros. Given the very small number of gaps, the influence of the gap filling
205 process is considered negligible. For Manaus, the data gaps were larger, and the procedure of gap
206 filling is identical to the LBA Data Model Intercomparison Project [de Gonçalves *et al.*, 2013].

207 **3 Methods**

208 The sensitivity of ecosystem responses in terms of water and carbon fluxes to the short temporal
209 scales (~1h) and the interannual variability of climate is assessed with a particular emphasis on
210 precipitation, temperature, and incoming shortwave radiation. The sensitivity is studied using
211 numerical simulations carried out with a state-of-the-science mechanistic ecohydrological model.
212 The general principle guiding the simulations is that synthetic climate time series with prescribed
213 statistical properties are used to drive the model, which yields responses that mimic ecosystem
214 responses to the changed forcing conditions. The model has been previously calibrated and
215 evaluated for several sites considered here and a summary of the evaluation for all of the sites is
216 included in the Supplementary Material. The total rainfall amount, total radiation, and long-term
217 temperature are preserved across runs for each site. The corresponding statistical distributions and
218 correlation structure in time are the variables that were synthetically varied here.

219 **3.1 Ecohydrological Model and Vegetation Representation**

220 The mechanistic ecohydrological model Tethys-Chloris (T&C) [Fatichi, 2010; Fatichi *et al.*,
221 2012a, 2012b] is employed because this model has been shown to reproduce satisfactorily the

222 fluxes of energy, carbon, and water across a wide range of temporal scales in many sites
223 worldwide [*Fatichi and Leuzinger, 2013; Fatichi and Ivanov, 2014; Fatichi et al., 2014a; Pappas*
224 *et al., 2015*]. Here, only a brief description of the model is provided for reference; the details of
225 its mathematical formulation can be found elsewhere [*Fatichi, 2010; Fatichi et al., 2012a*]. T&C
226 simulates the essential hydrological and ecological processes regulating the water and carbon
227 cycles. In particular, the model resolves the water and energy budgets at the soil and land surface
228 and also accounts for vegetation dynamics. Meteorological variables required by the model are
229 hourly time series of precipitation, temperature, incoming shortwave radiation, air temperature,
230 wind speed, cloudiness, relative humidity, and atmospheric pressure above the canopy.

231 The modeled hydrological processes include saturated and unsaturated soil water flow and
232 overland flow, interception, throughfall, snow hydrology, and a full solution of energy fluxes at
233 the land surface. The result of this solution is a detailed quantification of the water fluxes between
234 the soil/canopy and the atmosphere. The modeled pathways include: water flow in the soil
235 computed from Richards equation modified to include a distributed sink term representing root
236 uptake, and soil evaporation but without accounting for hydraulic redistribution. Soil depth and
237 root zone depth are model parameters assigned to best represent local pedology and vegetation
238 characteristics. Overland flow is estimated by solving the kinematic wave approximation of the
239 Saint Venant equation. Interception and throughfall are modeled as a function of precipitation
240 intensity and leaf area index. The solution of the energy balance, which also affects snow
241 accumulation and melt, is performed using a resistance scheme analogue [*Sellers et al., 1996*]. In
242 the present version of T&C, five resistances (atmospheric, under-canopy, soil, stomatal, and leaf
243 boundary) are used and only one radiative temperature is estimated per time step. Even though
244 T&C was developed to operate at the catchment scale and account for the influence of complex
245 topography on radiation distribution (e.g. shading) and lateral water flow, flat terrain is assumed
246 as a close approximation for all flux tower sites considered here.

247 T&C can use the concept of plant functional types (*PFTs*) or species specific parameters and
248 conceptualizes vegetation structure as a series of inter-connected carbon pools, a methodology
249 commonly used in dynamic global vegetation models [*Haxeltine and Prentice, 1996; Sitch et al.,*
250 *2003; Krinner et al., 2005a; Oleson et al., 2013*]. Biomass in various plant carbon pools (leaves,
251 fine roots, living sapwood, non-structural carbohydrates, etc.) is estimated in a prognostic manner
252 based on a system of differential equations that regulate carbon inputs (photosynthesis), losses
253 (respiration, tissue turnover), and translocation among them, which follow a set of allometric,
254 resource availability, and phenology status, rules. Photosynthesis is modeled using the widely

255 accepted biochemical model at the leaf scale presented by *Farquhar et al.*, [1980], including
256 some modifications [*Collatz et al.*, 1991; *Dai et al.*, 2004; *Kattge and Knorr*, 2007; *Bonan et al.*,
257 2011]. Photosynthesis can be reduced during drought stress periods, which are defined as periods
258 when the soil water potential drops below a plant specific threshold. This photosynthetic
259 reduction is based on a reduction factor that varies linearly with the soil moisture available to the
260 roots, which is a function of root and soil moisture vertical distributions. Intercepted water
261 inhibits transpiration [*Deardorff*, 1978] but does not inhibit CO₂ uptake except for the case when
262 the canopy is at least 50% covered with snow. Carbon maintenance and growth respiration fluxes
263 are modeled as a function of temperature, living biomass for every carbon pool and their carbon
264 to nitrogen ratio [*Krinner et al.*, 2005b; *Fatichi*, 2010]. Biomass allocation in leaves is translated
265 into a dynamic behavior of the leaf area index (LAI) based on the specific leaf area index, while
266 other plant characteristics, such as plant height and root distribution are maintained ‘static’.
267 Vegetation dynamics are affected by environmental forcing and are coupled with the main
268 hydrological processes. Soil biogeochemistry and nutrient cycles are not explicitly simulated,
269 thus the model assumes vegetation to be in equilibrium with its nutritional environment. A
270 detailed description of the model can be found elsewhere [*Fatichi*, 2010; *Fatichi et al.*, 2012a,
271 2012b].

272 Initial conditions (carbon pools and soil water) for all the model runs were selected such that they
273 represent realistic mature ecosystems in balance with their observed meteorological forcing, i.e.
274 they are in a quasi-steady-state equilibrium.

275 **3.2 Climate Forcing**

276 The main focus is on the effect of inter-annual and short scale (~1 hr) climate variability on water
277 and carbon fluxes. To conduct such an assessment, a series of synthetic climate inputs that
278 manipulate the statistical structure of precipitation, temperature, and radiation are used to drive
279 T&C. In particular, 12 different input cases are evaluated (Table 1), where the spectral and
280 probabilistic structure of the climatic variables and their coherence with other climatic drivers are
281 modified. The first case corresponds to the observed climate input and represents the benchmark,
282 referred to as the control scenario throughout the manuscript. In the next 2 of the 12 cases, we
283 simultaneously alter all climate forcing types, while in the remaining 9 cases, the effect of each of
284 the variables of interest is separately modified, preserving the consistency of the other climatic
285 variables with the measurements. Seasonality is a deterministic mode of temporal variability that
286 influences ecosystem functioning. In the present study, we eliminated this degree of freedom
287 from simulations and in all of the scenarios seasonal patterns of all climate variables are

288 guaranteed to be identical to the observed series. The simulation length for all the cases is set to
289 that of the observed series, and for the cases where random sampling was used, five ensembles
290 were simulated to mimic stochastic variability.

291 3.2.1 Combined cases

292 For the two cases where all climatic variables are simultaneously perturbed, the focus is on the
293 combined effect of small-scale variability and the correlation structure (i.e., autocorrelation and
294 cross-correlations among all climatic variables) of the input.

295 In the second case (Table 1), the interannual variability along with the short scale variability of
296 precipitation, temperature, and radiation are suppressed. This is achieved by forcing the model
297 with periodic input of the 3 variables of interest in which only the 2 dominant modes of
298 variability, the seasonal and the diurnal are retained so that:

$$C_h^m(t) = \frac{1}{n} \sum_{i=1}^n C_{oh}^m(i) \quad \text{Eq 1}$$

299 where $C_h^m(t)$ is the climate variable of the t –th time step corresponding to the m –th month and
300 h –th hour, and $C_{oh}^m(i)$ is the observed variable at the i –th time step corresponding to hour h
301 and month m , and n is the total number of time steps for a specific month and hour. This input
302 scenario serves as an indication as to whether carbon dynamics and water fluxes can be predicted
303 from the mean values of the climatic forcing. Moreover, it can illustrate the importance of the
304 overall climate variability for water and carbon fluxes.

305 In the third case, the correlation structure of the model input is altered by randomizing the 3
306 variables of interest (i.e., precipitation, temperature, and radiation) in time, specifically, using
307 sampling without replacement. Sampling without replacement is used since we seek to preserve
308 exactly the observed meteorological values without repetitions that would arise from sampling
309 with replacement. For this case, two subcases are taken into account. In the first subcase, we
310 randomize simultaneously in time all the 3 variables of interest. If $I = \{i_1, i_2, \dots, i_n\}$ are the time
311 indices of data to be randomized, the randomized series of precipitation, temperature, and
312 radiation are $P_r = P_o\{I_p\}$, $T_r = T_o\{I_p\}$, $R_r = R_o\{I_p\}$, where I_p is a random sample from I ,
313 P_r, T_r, R_r are the randomized series, and P_o, T_o, R_o are the observed series of precipitation,
314 temperature and radiation respectively. In the second subcase the randomized series are $P_r =$
315 $P_o\{I_p^1\}$, $T_r = T_o\{I_p^2\}$, $R_r = R_o\{I_p^3\}$, where I_p^1, I_p^2, I_p^3 are 3 different samples from I . In the first
316 case, the autocorrelation of the 3 climate variables are destroyed, but their conditional probability

317 distributions are preserved. In the second subcase, the autocorrelation in time and the cross-
318 correlations among precipitation, radiation and temperature are destroyed. However, note that to
319 maintain some realism in the input, the seasonal and diurnal cycles of the climatic input variables
320 are retained. To achieve that the sampling pool is restricted for every variable based on the month
321 and hour of the day is was observed.

322 3.2.2 Precipitation

323 The precipitation statistical structure is probably the most complex among the environmental
324 drivers. The main features of the small scale statistical structure of precipitation are its
325 intermittent nature, highly skewed distribution, and autocorrelation [Molini *et al.*, 2009;
326 Paschalis, 2013; Paschalis *et al.*, 2013, 2014a]. Event-scale precipitation structure affects the
327 amount and timing of available water in the rooting zone. Moreover, due to lagged effects of the
328 water flow within soil, the small scale variability of precipitation can influence plant water
329 availability over a much wider range of scales and potentially introduce long term effects on
330 ecosystem functioning [Katul *et al.*, 2007a]. Evidence of such long term effects has been
331 provided by experimental studies for semiarid regions [Swemmer *et al.*, 2007] and has been
332 hypothesized to play a role in the Amazon rainforest [Ivanov *et al.*, 2012b].

333 In this study, 4 precipitation scenarios that encompass many plausible conditions are considered.
334 In the first precipitation scenario (case 4 in Table 1), the correlation structure of precipitation is
335 perturbed by randomizing the observed hourly precipitation, while preserving seasonal and
336 diurnal patterns. The randomization of precipitation has two significant impacts on the
337 precipitation statistical structure. First, precipitation autocorrelation in time is destroyed, and
338 second, the distribution of coherent dry and wet spells is modified since precipitation clustering
339 into storm events does not occur anymore. The altered precipitation has statistically shorter inter-
340 and intra- storm durations. To isolate the effect of the correlation structure of precipitation from
341 amounts, the total precipitation annual amounts are set equal to the control scenario (i.e. the inter-
342 annual variability of precipitation is preserved).

343 In the second precipitation scenario (case 5), interannual variability of precipitation is removed
344 and precipitation series within year are standardized as:

$$R_s^i(t) = R^i(t) \frac{\overline{R_a}}{R_a^i}, \quad \text{Eq 2}$$

345 where $R_s^i(t)$ is the standardized precipitation depth for time t of the year i , $R^i(t)$ is the recorded
346 precipitation depth, R_a^i is the annual depth of the i -th year and $\overline{R_a}$ is the long term annual depth.

347 This scenario allows the estimation of the sole impact of the small-scale structure of precipitation,
348 which essentially remains intact, while the effects of the longer-term fluctuations are removed.

349 The third precipitation scenario (case 6) enhances precipitation peaks by employing the following
350 probability transform:

$$R_s^+(t) = F_g^{-1}(F[R^+(t)], a_g, b_g) \quad \text{Eq 3}$$

351 where $R_s^+(t)$ is the positive part of the synthetic precipitation, $F[\cdot]$ is the cumulative distribution
352 function of the positive part of the observed precipitation $R^+(t)$, and $F_g^{-1}[\cdot]$ is the inverse of the
353 cumulative distribution function of the Gamma distribution with parameters a_g and b_g . The
354 choice of such a cumulative distribution is based on prior studies demonstrating that precipitation
355 depths are reasonably approximated by a Gamma distribution [Papalexiou *et al.*, 2013; Paschalis
356 *et al.*, 2014a]. The parameters a_g and b_g parameters are estimated using the method of moments
357 (the first two moments are used). The mean value is set to be the same as the observed
358 precipitation, thereby preserving the amounts over long periods. The standard deviation is set to 4
359 times the observed value to amplify the peak magnitude. The synthetic precipitation time series
360 has the same intermittency pattern as the observed, the same mean value but, as expected, larger
361 peaks. This scenario is intended to reveal the potential of extreme high precipitation influencing
362 the water and carbon fluxes, which has been previously found to be important especially in water
363 limited ecosystems [Knapp *et al.*, 2008]. Similar to the first case, the annual totals of precipitation
364 are standardized to preserve interannual variability.

365 The fourth precipitation scenario (case 7) unfolds the significance of the storm event precipitation
366 depth. To separate the effect of the precipitation distribution within the event, and the potential
367 influence of its peaks, synthetic precipitation series are constructed using the following integral

$$R_s(t) = \frac{1}{\Delta} \int_{t-\Delta/2}^{t+\Delta/2} R(t) dt, \quad \text{Eq 4}$$

368 where, $R(t)$ and $R_s(t)$ are the observed and simulated precipitation depths respectively. Choosing
369 Δ comparable to a typical storm size, and smaller than the inter-storm period, the resulting
370 precipitation is structured in distinct precipitation events, with comparable cumulative
371 precipitation depths and durations to the observed ones (per storm), but reduced peaks. For all
372 sites, $\Delta = 12$ h is selected. This scenario reveals to what extent the precipitation amount of events
373 rather than the sub-event structure influence the functioning of the ecosystems [Heisler-White *et*
374 *al.*, 2008]. In this case, the inter-annual variability of precipitation is also preserved.

375 **3.2.3 Temperature**

376 In contrast to precipitation, air temperature fluctuations are dominated by the 2 dominant modes,
377 the seasonal and the diurnal, which explain much of the total air temperature variance. The rest of
378 the variability consists of high frequency fluctuations (hours-days) associated with weather
379 patterns and low frequency fluctuations (interannual and beyond) linked to phenomena such as
380 the El-Niño Southern oscillation [*Gu and Adler, 2011*].

381 Temperature variability is investigated at the hourly and the interannual scales. For this reason, 3
382 different scenarios are constructed. In the first scenario (case 8), the correlation pattern of
383 temperature at the hourly scale is altered: the series is randomized in the same fashion as for the
384 precipitation case 4, preserving the diurnal and seasonal patterns as well as the marginal
385 distribution of temperature. With this case, we explore whether persistence of temperature can
386 alter ecosystem functioning. Moreover, the effect of the cross-correlations of temperature with the
387 rest of the climatic forcing is also investigated, since cross-correlation is altered as well. To
388 isolate the effect of the short scale correlations, the mean annual temperatures are set equal to
389 those of the observed series to preserve interannual variability consistent with the measurements.

390 In the second temperature scenario (case 9), interannual variability of temperature is removed
391 using a procedure similar to Eq 2. In this case, the effect of the intra-annual variability of
392 temperature is isolated by removing the effects of long-term variations found to be significant in
393 temperature limited ecosystems [*Tian et al., 1998; Babst et al., 2013*].

394 Finally, a moving average filtering to the temperature series identical to Eq 4 is implemented for
395 the third temperature scenario (case 10). In this case, the distribution of the temperature is
396 modified by smoothing warm and cold fluctuations occurring over short periods, while keeping
397 the seasonal patterns of temperature unchanged. This case can reveal whether or not the
398 probability density function of temperature significantly impacts water and carbon fluxes. Since
399 the response of ecosystems to climatic forcing is in general non-linear, any reduction in
400 temperature extremes may have an impact, difficult to predict a priori, and is explored here. As
401 before, interannual variability of temperature is also preserved.

402 **3.2.4 Radiation**

403 The last climatic variable to be investigated is incoming shortwave radiation at the land-surface.
404 The statistics of the radiation time series are similar to that of temperature, with the two major
405 modes of variability being the seasonal and diurnal. Small-scale variability is linked to weather,
406 with cloud formation reducing the amount of direct radiation from its expected clear-sky value.

407 Large-scale interannual variability is relatively low, and can be associated with anthropogenic
408 aerosol emissions and volcanic eruptions [Wild *et al.*, 2005; Norris and Wild, 2007].

409 In the case of radiation, two different scenarios similar to the temperature cases are constructed.
410 In the first one (case 11), the correlation structure is removed but the observed radiation
411 interannual, seasonal, and daily variability are preserved; in the second radiation scenario (case
412 12), the interannual variability is removed.

413 **3.3 Statistical evaluation of the simulations**

414 The objective here is a systematic exploration of cross-scale information flow from small scale
415 climatic fluctuations to long-term carbon/water fluxes in various ecosystems. In particular, how
416 short-term variability in precipitation, air temperature, and incident radiation translates to
417 variability in water and carbon fluxes across temporal scales is explored.

418 **3.3.1 Interannual variability of water and carbon fluxes**

419 The effects of interannual and short scale temporal variability of hydrometeorologic forcing on
420 the “climatology” of *ET* and carbon assimilation are considered focusing on three aspects: (a) the
421 mean values at the annual scale, (b) their variance, and (c) the “shape” of interannual fluxes, i.e.,
422 the temporal pattern of the multi-year fluctuations. A scheme of the analysis approach for water
423 and carbon fluxes at the annual scale is presented in Figure 2. The three aspects are referenced to
424 the control scenario, which uses the measured meteorological inputs. The evaluation of potential
425 differences in the mean values and standard deviation for each scenario is presented (Figure 2).
426 The correlation coefficient between annual time series of the control simulation and the time
427 series obtained using the input scenarios is also investigated. This analysis provides a direct
428 metric of the relative impact of the perturbed meteorological forcing statistics in modifying inter-
429 annual variability of a given variable. In other words, given that each of the synthetic input
430 scenarios alters only one property of the interannual or short scale variability of the
431 meteorological input, the impact of that specific property on the inter-annual variability of the
432 water and carbon fluxes can be assessed as a reduced cross-correlation. The fluxes explored here
433 are: *ET*, the partition of *ET* into evaporation and transpiration, and gross primary production
434 *GPP*. We chose to analyze *GPP*, representing the gross carbon assimilation, rather than Net
435 Ecosystem exchange (*NEE*), which could be possibly a better descriptor of the total carbon
436 balance of each ecosystem due to the large uncertainties involved in the simulation (and
437 measurements) of ecosystem respiration components, especially those describing below ground
438 heterotrophic respiration [Vargas *et al.*, 2010].

3.3.2 Spectral analysis

To quantify the influence of each of the investigated characteristics of climate variability on the modeled water and carbon fluxes across scales, the coherence spectrum between two time series is employed. The squared coherence spectrum between two series $X(t)$ and $Y(t)$ is defined as:

$$C_{xy}(f) = \frac{|S_{xy}(f)|^2}{S_{xx}(f)S_{yy}(f)}, \quad \text{Eq 5}$$

where f is the frequency, $S_{xy}(f)$ is the cross spectral density between the two series, and $S_{xx}(f), S_{yy}(f)$ are the spectral densities of $X(t)$ and $Y(t)$, respectively. The $C_{xy}(f)$ is bounded (i.e., $[0,1]$). The coherence spectrum shows the similarity between $X(t)$ and $Y(t)$ in the frequency domain. It is therefore a suitable technique to analyze signals across a wide range of temporal scales. The coherence spectra are estimated using the Fast Fourier Transform (FFT) [Press et al., 1992; Baldocchi et al., 2000]. Post processing includes the use of a modified Welch's overlapped averaged periodogram method. All the calculations were performed in Matlab. Alternative estimations, which are based on the wavelet decomposition also exist, and are gaining popularity in data analysis and model comparisons in ecological and climate studies but are not used here [Torrence and Compo, 1998; Katul et al., 2001; Dietze et al., 2011; Stoy et al., 2013].

Coherence spectra of simulated variables are computed using the control simulation ($X(t)$) and each of the 12 input scenarios ($Y(t)$). The frequencies at which coherence exhibits low values can be interpreted as the temporal scales in which the influence of the modified characteristic of forcing variability is significant. Due to the system nonlinearities and feedbacks between the processes controlling the water and carbon cycles, it is not expected that the impact of perturbations of meteorological inputs that are imposed at the highest frequency (1 hour) will monotonically decrease with increasing temporal scales. The coherence spectra can be used as a tool to identify in which cases short scale temporal variability of the meteorological forcing has the potential to affect water and carbon at larger scales, e.g., at the inter-annual level (section 3.3.1), and provide clues to a mechanistic explanation as to why such dependencies occur. A caveat related to the coherence spectra analysis is that an assessment of the “signal similarity” at low frequencies is highly impacted by the length of the analyzed series. For this reason the linear correlation analysis described before can serve as a complementary analysis to the coherence spectra.

The scales in the coherence spectral analyses considered span from 1 hour (i.e., the frequency of the simulations) up to few months. Coherence estimates for coarser scales are unreliable due to

469 the limited simulation length, which is restricted by the meteorological data availability for each
470 site.

471 **4 Results and Discussion**

472 **4.1 Presentation of the results**

473 The results of the two types of analyses are presented – the correlation analysis that is
474 conceptually presented in Figure 2 and the squared-coherence analysis that emphasizes
475 information propagation across temporal scales from ‘forcing’ (3 climatic variables with various
476 statistical structure) to ‘response’ (mainly *ET* and *GPP*). Figures 3-4 present the outcome of the
477 correlation analysis for each ecosystem, emphasizing the interannual variability of the fluxes,
478 while Figures 5 to 8 suggest connections or interpretations between forcing and response
479 variables specific to a given ecosystem and across seasons expanding on the results shown in
480 Figures 3-4. Figure 9 summarizes the outcome of the squared coherence analysis across sites and
481 by response variable. Additional information that yield outcomes similar to the ones in the
482 aforementioned figures are only included in the Supplementary Material. For clarity, we report
483 only the first subcase of the perturbation 3 (Table 1) in all figures. In this subcase, precipitation,
484 temperature and radiation were randomized using the same time index, i.e., preserving the
485 covariance (section 3.2.1). For all fluxes and stations considered, there was not substantial
486 difference between the 2 subcases indicating that destroying the conditional probability
487 distributions between precipitation, temperature and radiation does not add much to the alteration
488 of their auto-correlations. For completeness, results from the second subcase are reported in the
489 Supplementary Material.

490 **4.2 Water-limited ecosystem (Lucky Hills)**

491 Lucky Hills site represents a water-limited ecosystem. The mean values of *ET* at the annual time
492 scales are almost equal for all input scenarios (Figure 3a). These findings are consistent with
493 expectations as the site is located in the water-limited regime where potential evapotranspiration
494 $PET > ET \approx P$ [Fatchi and Ivanov, 2014] according to the Budyko’s curve. Water losses due to
495 surface runoff and leakage to the deep soil layers are small for this location ($\approx 2\text{-}20 \text{ mm year}^{-1}$).
496 This fact explains the reason why the basic determinant of the shape of inter-annual fluctuations
497 of *ET* is the total annual precipitation depth. This finding is further illustrated by the low value of
498 the correlation coefficient between the annual fluxes of *ET* estimated for the control scenario, and
499 the case 5 with no inter-annual variability (IAV) of annual precipitation (Figure 3a).

500 Although precipitation variability does not influence the total annual *ET* flux, it affects the
501 partitioning between evaporation and transpiration (Figure 3c-d). Both the total amount of annual
502 precipitation and precipitation structure at short temporal scales impact the partition between
503 ground evaporation and transpiration because precipitation intensity affects interception and soil
504 moisture vertical distribution. This has a net effect on the composition of the *ET* flux.

505 Scenarios that impose a loss in the internal correlation and intermittency structure of precipitation
506 (Figure 3c; cases 3-4) or a periodic input (Figure 3c; case 2) lead to increased evaporation from
507 interception and bare soil evaporation losses. The reason for larger evaporation from interception
508 is that when precipitation events are not sufficiently large (cases 2, 3, and 4), higher amounts of
509 water are intercepted by the canopy. The reason for enhanced bare soil evaporation is deemed to
510 be related to how precipitation wets the soil column. For water to penetrate deeper into the soil
511 and become available for root uptake, large precipitation pulses are required. In the absence of
512 well-structured precipitation events (i.e. precipitation events that last long to accumulate a
513 significant amount of water), infiltrated water is mostly in the top soil layer and dissipated mostly
514 as evaporation from the soil surface.

515 The way precipitation structure determines water availability in the root zone subsequently affects
516 root access to water, and thus transpiration. As shown in Figure 3d (cases 2-4), when evaporation
517 becomes the dominant flux, less water is available for plant uptake and transpiration. Total
518 precipitation and precipitation structure are significant for determining transpiration at the annual
519 scale, as shown by the low values of the correlation coefficient between precipitation and
520 transpiration in Figure 3d (cases 2-4).

521 The way precipitation structure at the short temporal scales affects the partition of *ET* into its
522 components has been found to be similar in terms of patterns across all ecosystems analyzed. For
523 this reason, the partition discussed in detail for the case of Lucky Hills is not further repeated in
524 later sections. A detailed quantification of this effect is given in the Supplementary Material.

525 Annual total and precipitation structure at the finest temporal scales have also a major influence
526 on carbon assimilation. Due to the linkage between photosynthesis and transpiration through
527 stomatal conductance, the behavior of inter-annual variability of *GPP* is similar to that of
528 transpiration (Figure 3b). Short scale variability of precipitation affects root zone water content
529 and, specifically, the time fraction that vegetation is under water-stress (Figure 5) defined here as
530 the percentage of time during which the integrated soil water content in the root zone is below the
531 water content threshold at which stomata begin to close. Similar to transpiration, carbon

532 assimilation is lower whenever the soil water conditions are not favorable for vegetation over
533 longer periods. For the semi-arid location of Lucky Hills, this occurs when either the intermittent
534 nature of precipitation is not taken into account (i.e., input scenario with periodic precipitation),
535 or whenever discrete precipitation events (i.e., input scenario with no correlation structure) cannot
536 wet the root zone sufficiently deep (Figure 3b; cases 2-4). This result is also consistent with
537 previous modeling studies, which showed a significant dependence between the storm arrival
538 rates, the event precipitation depths, and vegetation productivity [Ridolfi *et al.*, 2000; Daly *et al.*,
539 2004; Porporato *et al.*, 2004].

540 An interesting feedback is the increase in leaf area index LAI due to enhanced GPP, which can
541 then lead to potential reductions in soil moisture. Enhanced GPP can lead to increased LAI,
542 which in turn increases water loss from interception (due to larger interception capacity) and
543 transpiration, thus creating less favorable soil water conditions for the plant. This feedback is
544 generally captured by the model but when it operates at longer multi-year scales, longer term
545 simulations and an explicit accounting of nutrient dynamics should be carried out, which is not
546 the case of this study.

547 How the short temporal scale perturbations in the precipitation time series affect the behavior of
548 water and carbon fluxes across a range of temporal scales, and how they impact ecosystem
549 performance at the annual scale is considered for the Lucky Hills site by analyzing the coherence
550 spectra. The first feature concerning the spectral analysis is the substantial difference of the shape
551 of the coherence spectra corresponding to the randomization of precipitation, temperature, or
552 radiation. The effect of the distortion of the short scale variability of radiation and temperature in
553 general seems to decrease with increasing scale, as illustrated by the increasing value of the
554 squared coherence with decreasing frequencies (Figure 9c-f). In contrast, the distortion of
555 precipitation structure at the highest frequency affects the behavior of the water and carbon fluxes
556 also at lower frequencies. The explanation for this behavior is that radiation and temperature
557 affect immediately (i.e., at the same time scale) the biochemical processes related to
558 photosynthesis and the biophysical process of evapotranspiration. Conversely, precipitation
559 structure at the finest scale can alter the availability of water in the root zone, which impacts
560 transpiration and *GPP*. The movement of water in the soil profile has a much longer characteristic
561 time scale (~days) in comparison to the imposed distortions at the short time scale by the
562 precipitation structure (hours) [Katul *et al.*, 2007a; Nakai *et al.*, 2014]. For this reason, lower
563 squared coherences occur at lower frequencies despite the distortion is only introduced at the
564 highest frequencies. This remarks the potential of the short scale variability of precipitation to

565 impact the behavior of carbon and water fluxes at much longer time scales. Temperature and
566 radiation, both in terms of annual means and short scale temporal structure, play only a minor role
567 on the ecosystem functioning since they rarely represent limiting factors.

568 The findings presented here provide mechanistic explanations of the importance of precipitation
569 pulse structure (amounts, organization, and recurrence) for ecosystem functioning, which has
570 been empirically observed in many semi-arid and desert ecosystems [Noy-Meir, 1973; Huxman *et al.*,
571 *et al.*, 2004b; Loik *et al.*, 2004; Nagler *et al.*, 2007; Williams *et al.*, 2009].

572 **4.3 Temperature-limited Ecosystem (UMBS)**

573 The second ecosystem investigated here is the deciduous forest located near the University of
574 Michigan Biological Station. The ecosystem is hypothesized to be primarily limited by low air
575 temperature and, to a smaller degree, by water and radiation.

576 *ET* at the annual time scale is primarily influenced by the short scale variability in precipitation,
577 and, to a less extent, by the temperature variability (Figure 4 a1, all cases). The shape of the IAV
578 of *ET*, expressed as the loss of correlation between the output of the control simulation and the
579 simulations with the considered scenarios, is influenced both by precipitation and temperature
580 variability. Specifically, the differences in the magnitude of *ET* at the annual time scale, which
581 are as high as 20% (Figure 4 a1, cases 3-12), are primarily driven by the abiotic process of
582 evaporation of water intercepted by the canopy and bare soil evaporation (See Supplementary
583 Material). Since UMBS is not in a water-limiting regime (based on the Budyko curve), *ET* is not
584 strictly limited by the total amount of annual precipitation (e.g., no loss of correlation for case 5).
585 However, *ET* can be sensitive to precipitation variability. The mechanisms that impact *ET* at the
586 annual time scale are due to precipitation interception by canopy, and bare soil evaporation from
587 the upper soil layer. The input scenarios leading to enhanced evaporation from soil and canopy
588 are the ones where precipitation is not structured in distinct events (Figure 4 a1, cases 2, 3, and 4).
589 Since soil water availability is limiting vegetation at the UMBS only rarely, changes in
590 transpiration flux have a minor influence on *ET* (Supplementary Material).

591 The mean annual gross primary production is essentially identical for all the forcing scenarios
592 with the exception of one where variability in all of the input types of forcing is neglected (Figure
593 4 b1, case 2). In particular, the loss of temperature variability at the shortest scale enhances
594 annual *GPP* (Figure 4 b1, case 2). The reason for this *GPP* enhancement is the nonlinear response
595 of photosynthesis to leaf temperature, where photosynthesis is defined here as the gross
596 assimilation of carbon per unit leaf area [Wohlfahrt and Gu, 2015], (Figure 6). Photosynthesis has

597 a steep increase with increasing temperature at low leaf temperatures and reaches a plateau
598 around the optimal temperature for carbon assimilation. Furthermore, the temperature distribution
599 at UMBS lies between the steep response regime and the plateau. This implies that time
600 averaging (indicated by the overline) results in $\overline{GPP(T_s)} < GPP(\bar{T}_s)$. At the UMBS, this
601 inequality is often satisfied during summer when productivity is maximum, and removing cold
602 spells (as done in case 2) results in a considerable enhancement of GPP . The contributions of
603 precipitation and radiation variability are negligible.

604 The shape of the IAV of GPP is almost uniquely determined by the mean annual temperature
605 (Figure 4b1, case 9). Standardization of the annual fluxes in terms of temperature leads to a
606 complete loss of correlation between the annual fluxes of GPP of the control and synthetic input
607 scenarios (case 9). Using the mean growing season temperature, rather than the mean annual
608 temperature, a more appropriate choice since the UMBS forest is deciduous does not affect the
609 finding, since the mean annual and the mean growing season temperature are highly correlated
610 (not shown here). Short temporal scale variability of temperature at the UMBS is unlikely to
611 influence the annual behavior of carbon fluxes since it does not result in long lasting effects (i.e.
612 no information transfer from small to large scales). Temperature variability at the shortest
613 temporal scale mostly affects the biochemical processes of photosynthesis that operate at the
614 same scale. This does not influence processes with long-memory (i.e., temperature effects are not
615 “stored” in the system), thus the impact of hourly temperature variability to the variability of GPP
616 across scales decreases rapidly with increasing temporal scale. An illustrated signature of this
617 finding is the increased squared coherence between GPP of the control input (case 1) and the
618 random input (case 8) at lower frequencies (Figure 9d). Temperature effects could potentially be
619 “stored” in the ecosystem, if plant reproduction would be considered (e.g. Carbon assimilation
620 affected by temperature in one year may influence the survival of the following offspring etc.).
621 However, since reproduction is neglected in present paper, further discussion is not provided.

622 **4.4 Radiation-limited Ecosystem (Manaus)**

623 The tropical rainforest located close to Manaus is an ecosystem expected to be primarily limited
624 by radiation availability, given the high temperatures throughout the year, the high precipitation,
625 and the longer root system that gives access to deep soil water (with the assumed root depth equal
626 to 10 m). The mean annual ET losses in Manaus are affected by the short scale temporal
627 variability of precipitation and temperature, but not by radiation (no change in annual magnitude
628 for cases 11 and 12). Similar to the UMBS site, the loss of short scale correlation in the forcing
629 series leading to unstructured rainfall without distinct storms (Figure 4a2; cases 2, 3, and 4)

630 results in higher *ET*, primarily due to abiotic contributions (see the Supplementary Material).
631 The reduction of precipitation peaks lead to higher *ET* due to the higher amount of water
632 intercepted by the canopy that can evaporate before reaching the ground. This effect is more
633 pronounced at this site due to the relatively high leaf area index (i.e. higher interception capacity)
634 and the year-long growing season, which both imply higher evaporation from interception
635 storage, when compared to the other sites. Even though precipitation and temperature variability
636 can influence the mean annual *ET*, they have no impact on the shape of the IAV of *ET*. In other
637 words, differences in the short scale precipitation or temperature structure can shift the time series
638 of the annual fluxes of *ET* without changing its shape.

639 Short scale temporal variability of radiation has no appreciable effect on the IAV of *ET*.
640 However, the mean annual incoming radiation affects the shape of the IAV of *ET*. This is
641 illustrated by the loss of correlation between annual fluxes of *ET* as modeled for the control
642 scenario, and input scenarios in which the IAV of incoming radiation is suppressed (Figure 4a2,
643 case 12).

644 The mean values of *GPP* are similar for all the input scenarios, except the scenario in which
645 variability of all of the meteorological parameters is neglected. In this case, *GPP* is enhanced
646 (~14%). The reason for this enhancement of *GPP* is similar to the one for the UMBS case related
647 to temperature, but in this case with radiation being the more limiting hydrometeorological
648 variable. Photosynthesis is affected in a nonlinear manner by incoming shortwave radiation and in
649 particular by *PAR* (photosynthetically active radiation over 400-700 nm wavelength range). In
650 tropical rainforests, overcast conditions occurring during wet seasons can substantially limit
651 photosynthesis. The dynamic effects of cloudiness cannot be captured when radiation variability
652 at the hourly scale is neglected (Figure 4b2, case 2). Furthermore, due to the concave nonlinearity
653 of the response of photosynthesis to incident *PAR*, it follows that $\overline{GPP(PAR)} < GPP(\overline{PAR})$ (see
654 also Medvigy et al., [2010]).

655 Similar to *ET*, the shape of the IAV of *GPP* is solely influenced by the mean annual magnitude of
656 incoming radiation. This influence is best illustrated by a low correlation coefficient between the
657 annual fluxes of *GPP* of the control scenario and the input scenario in which interannual
658 variability of incoming radiation is neglected (Figure 4b2, case 12). Short temporal scale
659 variability has no appreciable influence on the large temporal scale fluctuations in carbon
660 assimilation. The reason is that radiation influences photosynthesis almost immediately at short
661 scales and no residual contribution of such short scale radiation variability is retained at long time

662 scales. In other words, there is no considerable long-term “storage” of the radiation effects in this
663 ecosystem, for instance through changes in leaf area index (that is close to maximum here), forest
664 structure and composition (which are assumed static), or transpiration that would affect soil
665 moisture. The short scale discrepancies of *GPP* introduced through the short scale distortions in
666 the radiation series cannot propagate to larger temporal scales such as the IAV. An indication of
667 the reduction of influence of the short scale radiation variability on carbon and water fluxes is the
668 nearly monotonic increase of coherence with scale between the time series of *GPP* of the control
669 case and of the synthetic case 11 (Figure 9e-f). Due to the short range of frequencies for which
670 the coherence can be estimated (due to the limited amount of input data, Figure 9), we cannot
671 compute the behavior of coherence up to the annual scale.

672 **4.5 Co-limited Ecosystem (SMEAR II)**

673 The boreal forest in Finland is limited by two main environmental factors: low temperatures and
674 relatively low precipitation. Boreal forests are also known to be nitrogen limited but this
675 limitation is outside the scope of this study. The nitrogen limitation effects are partially accounted
676 for in the sensitivity of the maximum carboxylation capacity to temperature. However, the IAV of
677 the nitrogen cycle is not considered.

678 *ET* fluxes at the annual scale are influenced by the short scale variability of precipitation and
679 temperature, but are almost insensitive to radiation variability (no change in annual magnitude for
680 cases 11 and 12), even though the site is located at a high latitude and thus radiation is
681 theoretically a limiting resource for ecosystem functioning. Similarly to the sites considered
682 previously, input scenarios that disrupt precipitation structure, and especially its organization into
683 distinct storm events, generally lead to the enhanced *ET* fluxes, primarily due to abiotic
684 contributions (Figure 4a3). Further, a loss of correlation of the temperature at the hourly time
685 scale leads to a small decrease in *ET*. Notably, in terms of variability of *ET* fluxes at the annual
686 scale, most of the features of variability of precipitation and temperature contribute to the shape
687 of IAV of *ET*, as illustrated by the low correlation coefficients between the control simulation
688 and scenarios 3-10 (Figure 4a3). The most important features of precipitation forcing are its
689 correlation structure, its distribution - with emphasis on peaks, and the magnitude of annual
690 precipitation. In terms of temperature, the annual temperature and, to a smaller degree, the
691 temperature correlation structure at the fine temporal scales play a role in ecosystem *ET*. This
692 result illustrates that the predictive power of relations linking annual temperatures or annual
693 precipitation to the IAV of *ET* will perform very poorly for this site.

694 Carbon assimilation is also affected by both precipitation and temperature variability. In terms of
695 mean values, the loss of correlation structure of precipitation or temperature leads to a small
696 increase in *GPP* (up to 10%, case 3). Conversely, a decrease or an increase in precipitation peaks
697 leads to a small reduction in *GPP*. The reason for these responses is that the short scale temporal
698 variability of precipitation and temperature can influence soil water balance, and since water
699 availability may be limiting at this site, it can affect the duration during which vegetation is under
700 water stress (particularly during summer, Figure 7). The results from this site support the notion
701 that the effects of short scale variability in precipitation and temperature can propagate across
702 scales and influence the IAV of water and carbon fluxes, but only if mediated through a storage
703 term (e.g., through the water availability in the root zone).

704 **4.6 Non-limited Ecosystem (Duke Forest sites)**

705 A deciduous hardwood and an evergreen pine forests co-located within the Duke forest are
706 studied in the last analysis. For clarity, only the results for pine stand are presented due to their
707 similarities with the hardwood forest. Detailed results for the hardwood forest can be found in the
708 Supplementary Material. Temperatures in the Duke forest are reasonably high, such that they do
709 not hamper photosynthesis substantially during periods of leaf presence, and frost occurrence is
710 rare. Precipitation is sufficient to satisfy plant demand, with the exception of few intense but rare
711 drought events [Palmroth *et al.*, 2005]. Because of this, we characterize the system as ‘non-
712 limited’. In Duke forest, vegetation has been found to be mostly nitrogen limited [Oren *et al.*,
713 2001; Palmroth *et al.*, 2013] but since T&C does not simulate soil biogeochemistry and nitrogen
714 cycles, we cannot currently investigate the effect of this limitation.

715 The mean annual *ET* of the Duke forest is sensitive to both precipitation and air temperature
716 variability. In general, as was the case with the ecosystems considered previously, whenever
717 precipitation is not well structured into distinct events, bare soil evaporation and evaporation of
718 intercepted water from the canopy can substantially increase the total *ET* (Figure 4a4; cases 2-4).
719 The most important feature is that the loss of correlation of *ET* fluxes at the annual scale between
720 the control simulation and the rest of the scenarios is generally small. This finding suggests that
721 meteorological variability at the hourly or annual scale only marginally influences the shape of
722 the IAV of annual *ET* losses. In other word, the large-scale characteristics that are preserved
723 throughout all the simulations, such as the vegetation phenology, are the major determinants of
724 the shape of the IAV. The only cases in which there is some loss of correlation is when the IAV
725 of precipitation is neglected, or when the short scale precipitation structure is destroyed. In those
726 cases, the correlation coefficient can drop to ~0.7.

727 Similar to the annual *ET* fluxes, the mean *GPP* fluxes at the annual time scale are affected by
728 both the variability of precipitation and air temperature, even though the shape of IAV of these
729 fluxes is substantially unaffected (note the high correlation coefficient in Figure 4b4). In general,
730 differences in the magnitude of the mean value of *GPP* are below 10%. A common behavior in
731 both the pine and the hardwood stands is that disabling correlation, both in terms of precipitation
732 (Figure 4b; case 3) and temperature (Figure 4b; case 8), leads to higher *GPP*. When a loss of
733 correlation at the fine temporal scale for both variables is imposed, the results provide the highest
734 carbon assimilation. The reason for this small enhancement of *GPP* is that the loss of correlation
735 structure of precipitation and/or temperature at the highest frequencies tends to reduce the period
736 during which the ecosystem is water-stressed (Figure 8). Even though this time difference is
737 small, it occurs during the most productive period of the year, and thus translates to a non-
738 negligible difference in carbon assimilation.

739 **4.7 Synthesis**

740 The common mechanisms and their related physical processes linking the hydrometeorological
741 temporal variability to the variability in water and carbon fluxes and how short-term information
742 propagates to longer scales are summarized in the following. A schematic representation of the
743 relevant mechanisms is presented in Figure 10. Variability in precipitation, temperature, and
744 radiation can have either a direct or an indirect effect on (a) the rate of water infiltration in the
745 soil, (b) the biochemistry of carbon assimilation and (c) the partition of net radiation into sensible
746 and latent heat components.

747 Precipitation variability, and in particular its structure in well-organized events, affects directly
748 the partition of water into interception, near-surface soil water storage, deep-soil water storage,
749 and runoff. In general, precipitation organized in concentrated events leads to low interception by
750 the canopy and a strong percolation of water to deeper soil layers. Further, a large precipitation
751 depth or intense precipitation in a single event may lead to surface runoff. These differences in
752 water partition among the various water storage compartments subsequently (and indirectly)
753 affect the partition of net radiation into sensible and latent heat fluxes. Whenever a larger amount
754 of water is available at either the canopy surface or in the upper soil layer, the abiotic components
755 of evaporation (e.g. soil evaporation and evaporation from interception) are enhanced. This can
756 lead to a lower water availability in deeper soil and thus in the root zone. Water limitations in the
757 root zone may inhibit vegetation productivity and transpiration due to stomatal closure. The direct
758 effect of the water flux partitioning and the indirect effect on the energy balance occur at all of

759 the sites, while the indirect effect leading to vegetation productivity inhibition occurs only at the
760 water limited sites, where the soil water potential can drop below the stress threshold level.

761 Temperature and radiation variability can affect directly the biochemistry and the energy balance
762 of the ecosystem, and have the potential to indirectly affect the soil water availability.
763 Leaf/canopy photosynthesis depends non-linearly on both leaf temperature and absorbed
764 photosynthetic active radiation. Due to this reason, the distribution, rather than the correlation
765 properties of temperature and radiation, affect carbon assimilation. The lack of importance of the
766 correlation structure is due to the fact that photosynthesis is a fast process (i.e. responding in the
767 order of few minutes to temperature and radiation forcing) and thus it does not carry memory
768 effects. In our study, modifying temperature or radiation distributions had an influence only for
769 the sites where either temperature or radiation were limiting vegetation productivity (temperature
770 for UMBS, and SMEAR II; radiation for Manaus). The statistical distribution of temperature and
771 radiation (e.g. concentration in heat/cold waves, diurnal variability) modifies the relative
772 contributions of latent and sensible heat fluxes, and thus evaporation, transpiration, and the
773 distribution of leaf temperature. Such an impact has the potential to modify the soil water
774 availability and its vertical distribution in the soil profile, potentially affecting root water uptake
775 and vegetation productivity. This indirect influence of temperature and radiation on soil water
776 affects subsequently carbon assimilation only if it translates into periods of low soil water
777 moisture, and thus plant water stress. This was featured when water and temperature were
778 simultaneously a limiting factor (SMEAR II).

779 Given the relatively short time span of the simulation period, we did not investigate the dynamics
780 of nutrient limitations, species composition, forest demography (time scale ~years). However,
781 these are additional low frequency processes, which could potentially propagate information at
782 even longer time scales.

783 **4.8 Study limitations and perspectives**

784 The numerical analysis provided here has limitations that need to be discussed and form open
785 questions for future research.

786 First of all, the results are based on model simulations only, which have inherent assumptions and
787 depend on the model structure. Perhaps the most important limitation of the current generation of
788 ecohydrological and global dynamic vegetation models is the lack of a commonly accepted
789 mechanistic representation of vegetation growth and stress, mineral nutrition, and long-term
790 forest demography (mortality, recruitment, seedling survival) [*Moorcroft, 2006; Fisher et al.,*

791 2010; Pappas *et al.*, 2013; Xu *et al.*, 2013; Fatichi *et al.*, 2014b; Körner, 2015]. As a result, large
792 discrepancies have been identified in a number of model inter-comparison projects [Dietze *et al.*,
793 2011; McDowell *et al.*, 2013; Stoy *et al.*, 2013]. T&C has been found to reproduce well carbon
794 and water fluxes across temporal scales for many ecosystems (including those considered in this
795 study). However, interpretations should be considered with necessary caution. The most
796 important components of ecosystem functioning that are not handled in T&C are (1) detailed soil
797 biochemistry/plant mineral nutrition, (2) root adaptations to water and mineral resource
798 limitations, (3) internal plant hydraulics, (4) forest demography, and (5) hydraulic redistribution.
799 The first component can potentially provide additional limitations to plant growth and carbon
800 assimilation. One should note that it also represents a poorly constrained component in carbon
801 cycle modeling [Todd-Brown *et al.*, 2014]. The second component could add a further restriction
802 in the interpretation of the results, given that the time scales of root adjustments are comparable
803 with the simulation length [Joslin *et al.*, 2000; Yuan and Chen, 2010]. The third component may
804 be important for regulating sub-daily stomatal conductance and water stress but its importance
805 decreases for longer temporal scales [Bohrer *et al.*, 2005]. The fourth component is typically
806 relevant for time scales larger than ~20 years, but could possibly reflect on our results since
807 during a “good year”, plants can invest excess carbon to enhanced reproduction, affecting the
808 survival rates of the next offspring, and thus add an additional influence to the ecosystem
809 functioning [Peters, 2000; Reichmann *et al.*, 2013]. Additionally, during a “bad” year, increased
810 mortality can also affect the ecosystem dynamics with long-lasting effects. The last component is
811 receiving significant attention across a wide range of ecosystems (grasses to plantation forestry)
812 and climates (temperate, mesic and arid), as reviewed elsewhere [Caldwell and Richards, 1986;
813 Mendel *et al.*, 2002; Amenu and Kumar, 2008; Siqueira *et al.*, 2009; Neumann and Cardon, 2012;
814 Volpe *et al.*, 2013; Manoli *et al.*, 2014], but its significance at the ecosystem scale is hard to
815 establish because of limited observations.

816 Second, the input scenarios for this analysis correspond to synthetic cases in which input
817 variables have been constructed to preserve specific statistical characteristics. The choices were
818 dictated by the goal of investigating individual aspects such as short-term or IAV of precipitation,
819 temperature, and radiation without confounding effects. In this sense, the constructed scenarios
820 cannot strictly correspond to realistic observable cases, but are rather intended to provide results
821 concerning ecosystem functioning that can be unfolded from natural variability in
822 hydrometeorological forcing. Frameworks for generating more realistic hydrometeorological
823 forcing exist and rely on stochastic weather generators [Fatichi *et al.*, 2011; Paschalis *et al.*,

824 2013] that can be also tuned to reproduce the findings of the latest climate research, integrating
825 also the effect of anthropogenic CO₂ emissions.

826 Finally, while diverse in vegetation type and climatic conditions, the number of ecosystems
827 considered here is limited and falls short of providing a general picture of all ecosystem
828 functions. To assess the global effect of short-term climatic variability on water and carbon fluxes
829 worldwide, a similar framework can be replicated in a global model or calibrating the model in
830 the entire dataset of observation networks such as FluxNet [Wilson *et al.*, 2002; Bonan *et al.*,
831 2012].

832 **5 Conclusions**

833 The effect of short temporal scale (hourly-scale) and inter-annual variability of precipitation,
834 temperature, and radiation on the water and carbon fluxes for six ecosystems representing a range
835 of hydrometeorologic conditions has been explored. Numerical experiments were constructed in
836 which one key feature of the variability of the three major meteorological variables was perturbed
837 or statistically distorted from its observational (or reference) record. Subsequently a state-of-the-
838 science mechanistic ecohydrological model was used as a process-based “filter” to link each of
839 the perturbed climatic variables to ecosystem performance in terms of water and carbon fluxes.
840 Based on results of these simulations, the effects of each distinct feature of the meteorological
841 variability were analyzed. In particular, we focused on the interannual variability of *ET* and *GPP*.
842 With aid of spectral analysis, we highlighted the manner in which small-scale temporal variability
843 of hydro-meteorological input propagates across scales to alter the ecosystem response in terms
844 of water and carbon cycles.

845 The most significant result is that short-scale variability of hydrometeorological forcing can
846 impact carbon and water fluxes across a range of temporal scales, being primarily linked to the
847 main resource limiting a given ecosystem. In particular:

848 (a) Precipitation structure at the fine temporal scales and, specifically, its intermittency impact the
849 interannual variability of *ET* across all sites. Whenever water is not a strong limiting factor,
850 significant effects on annual *ET* magnitude occur due to changes in various statistical components
851 of the precipitation structure. Further, these changes cause significant impact on *ET* partition
852 between evaporation and transpiration across all the sites, with the influence of abiotic processes
853 playing the major role. This result demonstrates the fundamental role of the so called ‘pulse

854 structure' of precipitation, and illustrates its importance across all ecosystems, not necessarily
855 constrained to water-limited regimes.

856 (b) Temperature variability can affect water and carbon fluxes only in ecosystems where
857 temperature is a major limiting factor for the leaf-level biochemical processes, thus affecting
858 carbon assimilation. Since photosynthesis responds at the same time scale as fine-scale
859 fluctuations of temperature, short-scale variability in temperature can affect the total annual
860 carbon assimilation, but the long-scale fluctuations of carbon fluxes (expressed in this study as
861 the shape of interannual fluxes of *GPP*) are primarily affected by the long-scale fluctuations of
862 temperature (e.g., its interannual variability). Short scale temporal variability of air temperature
863 can affect the shape of inter-annual fluxes of *GPP* only if it can affect the root zone soil water
864 availability and increase or decrease the duration of water-stress periods. This occurs when co-
865 limitation of water and temperature takes place.

866 (c) Radiation variability can affect water and carbon fluxes in a similar manner to temperature.
867 Radiation affects evaporation, transpiration, and photosynthesis at the highest frequency regime,
868 and for this reason, radiation variability at the shortest scale does not influence the low frequency
869 responses of water and carbon fluxes (e.g., inter-annual variability), which may be instead
870 affected by the low frequency fluctuations of the radiative forcing, in radiation limited sites.

871 **Supplementary Material**

872 In the supplementary material accompanying this article, we provide the results for inter-annual
873 variability for *ET*, Evaporation, Transpiration, Gross and Aboveground Net Primary Production
874 across all the sites in tabulated form, and a series of figures presenting model validation for each
875 location.

876 **Acknowledgements**

877 We would like to thank the Editor Prof. Desai, and the two anonymous reviewers for their
878 comments that significantly improved our manuscript. The authors are grateful to all individuals
879 of the FLUXNET project (<http://fluxnet.ornl.gov/>) and the University of Michigan Biological
880 Station (<http://umbs.lsa.umich.edu/research/>) involved in the collection of the data used in this
881 study. A. Paschalis acknowledges the financial support of the Swiss National Sciences
882 Foundation (grant No P2EZP2_152244) and the Stavros Niarchos Foundation, through the SNSF
883 Early Postdoc Mobility Fellowship. G. Katul acknowledges support from the National Science
884 Foundation (NSF-AGS-1102227 and NSF-EAR-1344703), the United States Department of

885 Agriculture (2011-67003-30222), and the U.S. Department of Energy (DOE) through the Office
886 of Biological and Environmental Research (BER) Terrestrial Carbon Processes (TCP) program
887 (DE-SC0006967 and DE-SC0011461). V. Ivanov was supported by the NSF grant EAR 1151443.

Author Manuscript

References

- Allan, R. P., and B. J. Soden (2008), Atmospheric warming and the amplification of precipitation extremes., *Science*, 321, 1481–1484, doi:10.1126/science.1160787.
- Amenu, G. G., and P. Kumar (2008), A model for hydraulic redistribution incorporating coupled soil-root moisture transport, *Hydrol. Earth Syst. Sci.*, 12(1), 55–74, doi:10.5194/hess-12-55-2008.
- Araújo, A. C. et al. (2002), Comparative measurements of carbon dioxide fluxes from two nearby towers in a central Amazonian rainforest: The Manaus LBA site, *J. Geophys. Res.*, 107(D20), 8090, doi:10.1029/2001JD000676.
- Arora, V. K. et al. (2013), Carbon-concentration and carbon-climate feedbacks in CMIP5 earth system models, *J. Clim.*, 26(15), 5289–5314, doi:10.1175/JCLI-D-12-00494.1.
- Asseng, S., I. Foster, and N. C. Turner (2011), The impact of temperature variability on wheat yields, *Glob. Chang. Biol.*, 17(2), 997–1012, doi:10.1111/j.1365-2486.2010.02262.x.
- Babst, F. et al. (2013), Site- and species-specific responses of forest growth to climate across the European continent, *Glob. Ecol. Biogeogr.*, 22(6), 706–717, doi:10.1111/geb.12023.
- Baldocchi, D., E. Falge, and K. Wilson (2000), A spectral analysis of biosphere-atmosphere trace gas flux densities and meteorological variables across hour to multi-year time scales, *Agric. For. Meteorol.*, 2915, 1–27.
- Baldocchi, D. et al. (2001), FLUXNET : A new tool to study the temporal and spatial variability of ecosystem-scale carbon dioxide , water vapor , and energy flux densities, *Bull. Am. Meteorol. Soc.*, 82(4), 2415–2434.
- De Boeck, H. J., F. E. Dreesen, I. A. Janssens, and I. Nijs (2010), Climatic characteristics of heat waves and their simulation in plant experiments, *Glob. Chang. Biol.*, 16(7), 1992–2000, doi:10.1111/j.1365-2486.2009.02049.x.
- Boer, G. J. (2009), Changes in interannual variability and decadal potential predictability under global warming, *J. Clim.*, 22(11), 3098–3109, doi:10.1175/2008JCLI2835.1.
- Bohrer, G., H. Mourad, T. a. Laursen, D. Drewry, R. Avissar, D. Poggi, R. Oren, and G. G. Katul (2005), Finite element tree crown hydrodynamics model (FETCH) using porous media flow within branching elements: A new representation of tree hydrodynamics, *Water Resour. Res.*, 41(11), doi:10.1029/2005WR004181.
- Bonan, G. B. (2008), Forests and climate change: forcings, feedbacks, and the climate benefits of forests., *Science*, 320(5882), 1444–1449, doi:10.1126/science.1155121.
- Bonan, G. B., P. J. Lawrence, K. W. Oleson, S. Levis, M. Jung, M. Reichstein, D. M. Lawrence, and S. C. Swenson (2011), Improving canopy processes in the Community Land Model version 4 (CLM4) using global flux fields empirically inferred from FLUXNET data, *J. Geophys. Res.*, 116(G2), G02014, doi:10.1029/2010JG001593.

- Bonan, G. B., K. W. Oleson, R. a. Fisher, G. Lasslop, and M. Reichstein (2012), Reconciling leaf physiological traits and canopy flux data: Use of the TRY and FLUXNET databases in the Community Land Model version 4, *J. Geophys. Res. Biogeosciences*, 117(G2), doi:10.1029/2011JG001913.
- Brooks, P. D., P. A. Troch, M. Durcik, E. Gallo, and M. Schlegel (2011), Quantifying regional scale ecosystem response to changes in precipitation: Not all rain is created equal, *Water Resour. Res.*, 47(10), doi:10.1029/2010WR009762.
- Caldwell, M., and J. Richards (1986), Competing root systems: morphology and models of absorption, in *On the economy of plant form and Function*, pp. 251–273, Cambridge University Press.
- Cattiaux, J., H. Douville, R. Schoetter, S. Parey, and P. Yiou (2015), Projected increase in diurnal and interdiurnal variations of European summer temperatures, *Geophys. Res. Lett.*, 42(3), 899–907, doi:10.1002/2014GL062531.
- Collatz, G., J. Ball, C. Grivet, and J. Berry (1991), Physiological and environmental regulation of stomatal conductance, photosynthesis and transpiration: a model that includes a laminar boundary layer, *Agric. For. Meteorol.*, 54(1074), 107–136.
- Collatz, G., L. Bounoua, D. Randall, I. Fung, and P. Sellers (2000), A mechanism for the influence of vegetation on the response of the diurnal temperature range to changing climate Collatz in, *Geophys. Res. Lett.*, 27(20), 3381–3384.
- Curtis, P., C. Vogel, C. Gough, H. Schmid, H. Su, and B. Bovard (2005), Respiratory carbon losses and the carbon-use efficiency of a northern hardwood forest, 1999–2003, *New Phytol.*, 617(2), 437–456, doi:10.1111/j.1469-8137.2005.01438.x.
- Dai, Y., R. Dickinson, and Y. Wang (2004), A two-big-leaf model for canopy temperature, photosynthesis, and stomatal conductance, *J. Clim.*, 17, 2281–2299.
- Daly, E., A. Porporato, and I. Rodríguez-Iturbe (2004), Coupled dynamics of photosynthesis, transpiration, and soil water balance. Part I: Upscaling from hourly to daily level, *J. Hydrometeorol.*, 5(3), 546–558.
- Deardorff, J. W. (1978), Efficient prediction of ground surface temperature and moisture, with inclusion of a layer of vegetation, *J. Geophys. Res.*, 83(C4), 1889, doi:10.1029/JC083iC04p01889.
- Dietze, M. C. et al. (2011), Characterizing the performance of ecosystem models across time scales: A spectral analysis of the North American Carbon Program site-level synthesis, *J. Geophys. Res.*, 116(G4), G04029, doi:10.1029/2011JG001661.
- Donohue, R. J., M. L. Roderick, and T. R. McVicar (2007), On the importance of including vegetation dynamics in Budyko's hydrological model, *Hydrol. Earth Syst. Sci.*, 11(2), 983–995, doi:10.5194/hess-11-983-2007.
- Eagleson, P. (1978), Climate, soil, and vegetation: 1. Introduction to water balance dynamics, *Water Resour. Res.*, 14(5), 705–712.

- Fang, J., S. Piao, Z. Tang, C. Peng, and W. Ji (2001), Interannual variability in net primary production and precipitation., *Science*, 293, 1723, doi:10.1126/science.293.5536.1723a.
- Farquhar, G., S. Caemmerer, and J. Berry (1980), A biochemical model of photosynthetic CO₂ assimilation in leaves of C₃ species, *Planta*, 90, 78–90.
- Fatichi, S. (2010), The modeling of hydrological cycle and its interaction with vegetation in the framework of climate change, University of Florence, University Braunschweig.
- Fatichi, S., and V. Ivanov (2014), Interannual variability of evapotranspiration and vegetation productivity, *Water Resour. Res.*, 50(4), 3275–3294, doi:10.1002/2013WR015044.
- Fatichi, S., and S. Leuzinger (2013), Reconciling observations with modeling: The fate of water and carbon allocation in a mature deciduous forest exposed to elevated CO₂, *Agric. For. Meteorol.*, 174-175, 144–157, doi:10.1016/j.agrformet.2013.02.005.
- Fatichi, S., V. Y. Ivanov, and E. Caporali (2011), Simulation of future climate scenarios with a weather generator, *Adv. Water Resour.*, 34(4), 448–467, doi:10.1016/j.advwatres.2010.12.013.
- Fatichi, S., V. Y. Ivanov, and E. Caporali (2012a), A mechanistic ecohydrological model to investigate complex interactions in cold and warm water-controlled environments: 1. Theoretical framework and plot-scale analysis, *J. Adv. Model. Earth Syst.*, 4(2), 1–31, doi:10.1029/2011MS000086.
- Fatichi, S., V. Y. Ivanov, and E. Caporali (2012b), A mechanistic ecohydrological model to investigate complex interactions in cold and warm water-controlled environments: 2. Spatiotemporal analyses, *J. Adv. Model. Earth Syst.*, 4(2), 1–22, doi:10.1029/2011MS000087.
- Fatichi, S., M. J. Zeeman, J. Fuhrer, and P. Burlando (2014a), Ecohydrological effects of management on subalpine grasslands: From local to catchment scale, *Water Resour. Res.*, 50(1), 148–164, doi:10.1002/2013WR014535.
- Fatichi, S., S. Leuzinger, and C. Körner (2014b), Moving beyond photosynthesis: from carbon source to sink-driven vegetation modeling, *New Phytol.*, 201(4), 1086–2095, doi:10.1111/nph.12614.
- Fatichi, S., P. Molnar, T. Mastrotheodoros, and P. Burlando (2015), Diurnal and seasonal changes in near-surface humidity in a complex orography, *J. Geophys. Res. Atmos.*, 120, 2358–2374, doi:10.1002/2014JD022537.Received.
- Fay, P. a., J. D. Carlisle, A. K. Knapp, J. M. Blair, and S. L. Collins (2000), Altering Rainfall Timing and Quantity in a Mesic Grassland Ecosystem: Design and Performance of Rainfall Manipulation Shelters, *Ecosystems*, 3(3), 308–319, doi:10.1007/s100210000028.
- Fay, P. A., J. M. Blair, M. D. Smith, J. B. Nippert, J. D. Carlisle, and A. K. Knapp (2011), Relative effects of precipitation variability and warming on tallgrass prairie ecosystem function, *Biogeosciences*, 8(10), 3053–3068, doi:10.5194/bg-8-3053-2011.
- Fisher, R., N. McDowell, D. Purves, P. Moorcroft, S. Sitch, P. Cox, C. Huntingford, P. Meir, and F. I. Woodward (2010), Assessing uncertainties in a second-generation dynamic vegetation model caused

by ecological scale limitations., *New Phytol.*, 187(3), 666–81, doi:10.1111/j.1469-8137.2010.03340.x.

- Friedlingstein, P., M. Meinshausen, V. K. Arora, C. D. Jones, A. Anav, S. K. Liddicoat, and R. Knutti (2014), Uncertainties in CMIP5 climate projections due to carbon cycle feedbacks, *J. Clim.*, 27(2), 511–526, doi:10.1175/JCLI-D-12-00579.1.
- De Gonçalves, L. G. G. et al. (2013), Overview of the Large-Scale Biosphere–Atmosphere Experiment in Amazonia Data Model Intercomparison Project (LBA-DMIP), *Agric. For. Meteorol.*, 182-183, 111–127, doi:10.1016/j.agrformet.2013.04.030.
- Gonzalez, P., R. P. Neilson, J. M. Lenihan, and R. J. Drapek (2010), Global patterns in the vulnerability of ecosystems to vegetation shifts due to climate change, *Glob. Ecol. Biogeogr.*, 19(6), 755–768, doi:10.1111/j.1466-8238.2010.00558.x.
- Gough, C., B. Hardiman, L. Nave, G. Bohrer, K. D. Maurer, C. S. Vogel, K. J. Nadelhoffer, and P. S. Curtis (2013), Sustained carbon uptake and storage following moderate disturbance in a Great Lakes forest, *Ecol. Appl.*, 23(5), 1202–1215, doi:10.1890/12-1554.1.
- Gough, C. M., C. S. Vogel, H. P. Schmid, and P. S. Curtis (2008), Controls on annual forest carbon storage: Lessons from the past and predictions for the future, *Bioscience*, 58(7), 609–622, doi:10.1641/B580708.
- Gu, G., and R. F. Adler (2011), Precipitation and Temperature Variations on the Interannual Time Scale: Assessing the Impact of ENSO and Volcanic Eruptions, *J. Clim.*, 24(9), 2258–2270, doi:10.1175/2010JCLI3727.1.
- Haxeltine, A., and I. Prentice (1996), BIOME3: An equilibrium terrestrial biosphere model based on ecophysiological constraints, resource availability, and competition among plant functional types, *Global Biogeochem. Cycles*, 10(4), 693–709.
- He, L., V. Ivanov, G. Bohrer, J. E. Thomsen, C. S. Vogel, and M. Moghaddam (2013), Temporal dynamics of soil moisture in a northern temperate mixed successional forest after a prescribed intermediate disturbance, *Agric. For. Meteorol.*, 180, 22–33, doi: 10.1016/j.agrformet.2013.04.014.
- Heisler-White, J. L., A. K. Knapp, and E. F. Kelly (2008), Increasing precipitation event size increases aboveground net primary productivity in a semi-arid grassland., *Oecologia*, 158(1), 129–140, doi:10.1007/s00442-008-1116-9.
- Hutyra, L. R., J. W. Munger, S. R. Saleska, E. Gottlieb, B. C. Daube, A. L. Dunn, D. F. Amaral, P. B. de Camargo, and S. C. Wofsy (2007), Seasonal controls on the exchange of carbon and water in an Amazonian rain forest, *J. Geophys. Res.*, 112(G3), G03008, doi:10.1029/2006JG000365.
- Huxman, T. E. et al. (2004a), Convergence across biomes to a common rain-use efficiency., *Nature*, 429, 651–654, doi:10.1038/nature02561.
- Huxman, T. E., K. A. Snyder, D. Tissue, A. J. Leffler, K. Ogle, W. T. Pockman, D. R. Sandquist, D. L. Potts, and S. Schwinning (2004b), Precipitation pulses and carbon fluxes in semiarid and arid ecosystems., *Oecologia*, 141(2), 254–268, doi:10.1007/s00442-004-1682-4.

- IPCC (2013), Climate Change 2013 The physical science basis working group I Contribution to the fifth assessment report of the Intergovernmental Panel on Climate Change, Cambridge University Press.
- Ivanov, V. Y., R. L. Bras, and E. R. Vivoni (2008), Vegetation-hydrology dynamics in complex terrain of semiarid areas: 1. A mechanistic approach to modeling dynamic feedbacks, *Water Resour. Res.*, *44*(3), W03429, doi:10.1029/2006WR005588.
- Ivanov, V. Y., S. Fatichi, G. D. Jenerette, J. F. Espeleta, P. a. Troch, and T. E. Huxman (2010), Hysteresis of soil moisture spatial heterogeneity and the “homogenizing” effect of vegetation, *Water Resour. Res.*, *46*(9), W09521, doi:10.1029/2009WR008611.
- Ivanov, V. Y., L. R. Hutrya, S. C. Wofsy, J. W. Munger, S. R. Saleska, R. C. de Oliveira, and P. B. de Camargo (2012a), Root niche separation can explain avoidance of seasonal drought stress and vulnerability of overstory trees to extended drought in a mature Amazonian forest, *Water Resour. Res.*, *48*(12), W12507, doi:10.1029/2012WR011972.
- Ivanov, V. Y., L. R. Hutrya, S. C. Wofsy, J. W. Munger, S. R. Saleska, R. C. de Oliveira, and P. B. de Camargo (2012b), Root niche separation can explain avoidance of seasonal drought stress and vulnerability of overstory trees to extended drought in a mature Amazonian forest, *Water Resour. Res.*, *48*(12), W12507, doi:10.1029/2012WR011972.
- Jentsch, A., J. Kreyling, and C. Beierkuhnlein (2007), A new generation of climate-change experiments: events, not trends, *Front. Ecol. Environ.*, *5*(7), 365–374, doi:10.1890/1540-9295(2007)5[365:ANGOCE]2.0.CO;2.
- Joslin, J., M. Wolfe, and P. Hanson (2000), Effects of altered water regimes on forest root systems, *New Phytol.*, *147*(1), 117–129, doi:10.1046/j.1469-8137.2000.00692.x.
- Karl, T., R. Knight, and N. Plummer (1995), Trends in high-frequency climate variability in the twentieth century, *Nature*, *377*, 217–220.
- Kattge, J., and W. Knorr (2007), Temperature acclimation in a biochemical model of photosynthesis: a reanalysis of data from 36 species., *Plant. Cell Environ.*, *30*(9), 1176–90, doi:10.1111/j.1365-3040.2007.01690.x.
- Katul, G. G., C. T. Lai, K. Schäfer, B. Vidakovic, J. Albertson, D. Ellsworth, and R. Oren (2001), Multiscale analysis of vegetation surface fluxes: from seconds to years, *Adv. Water Resour.*, *24*(9-10), 1119–1132, doi:10.1016/S0309-1708(01)00029-X.
- Katul, G. G., A. Porporato, E. Daly, A. C. Oishi, H.-S. Kim, P. C. Stoy, J.-Y. Juang, and M. B. Siqueira (2007a), On the spectrum of soil moisture from hourly to interannual scales, *Water Resour. Res.*, *43*(5), doi:10.1029/2006WR005356.
- Katul, G. G., A. Porporato, and R. Oren (2007b), Stochastic Dynamics of Plant-Water Interactions, *Annu. Rev. Ecol. Evol. Syst.*, *38*(1), 767–791, doi:10.1146/annurev.ecolsys.38.091206.095748.
- Kayler, Z. E., H. J. De Boeck, S. Fatichi, J. M. Grünzweig, L. Merbold, C. Beier, N. McDowell, and J. S. Dukes (2015), Experiments to confront the environmental extremes of climate change, *Front. Ecol. Environ.*, *13*(4), 219–225, doi:10.1890/140174.

- Keefer, T. O., M. S. Moran, and G. B. Paige (2008), Long-term meteorological and soil hydrology database, Walnut Gulch Experimental Watershed, Arizona, United States, *Water Resour. Res.*, 44(5), doi:10.1029/2006WR005702.
- Kharin, V. V., F. W. Zwiers, X. Zhang, and M. Wehner (2013), Changes in temperature and precipitation extremes in the CMIP5 ensemble, *Clim. Change*, 119(2), 345–357, doi:10.1007/s10584-013-0705-8.
- Kim, Y., R. G. Knox, M. Longo, D. Medvigy, L. R. Hutyyra, E. H. Pyle, S. C. Wofsy, R. L. Bras, and P. R. Moorcroft (2012), Seasonal carbon dynamics and water fluxes in an Amazon rainforest, *Glob. Chang. Biol.*, 18(4), 1322–1334, doi:10.1111/j.1365-2486.2011.02629.x.
- Knapp, A. K., and M. D. Smith (2001), Variation among biomes in temporal dynamics of aboveground primary production., *Science*, 291(5503), 481–484, doi:10.1126/science.291.5503.481.
- Knapp, A. K. et al. (2008), Consequences of More Extreme Precipitation Regimes for Terrestrial Ecosystems, *Bioscience*, 58(9), 811–821, doi:10.1641/B580908.
- Kolari, P., J. Pumpanen, U. Rannik, H. Ilvesniemi, P. Hari, and F. Berninger (2004), Carbon balance of different aged Scots pine forests in Southern Finland, *Glob. Chang. Biol.*, 10(7), 1106–1119, doi:10.1111/j.1365-2486.2004.00797.x.
- Körner, C. (2009), Responses of humid tropical trees to rising CO₂, *Annu. Rev. Ecol. Evol. Syst.*, 40(1), 61–79, doi:10.1146/annurev.ecolsys.110308.120217.
- Körner, C. (2015), Paradigm shift in plant growth control, *Curr. Opin. Plant Biol.*, 25, 107–114, doi:10.1016/j.pbi.2015.05.003.
- Krinner, G., N. Viovy, N. de Noblet-Ducoudré, J. Ogée, J. Polcher, P. Friedlingstein, P. Ciais, S. Sitch, and I. C. Prentice (2005a), A dynamic global vegetation model for studies of the coupled atmosphere-biosphere system, *Global Biogeochem. Cycles*, 19, GB1015, doi:10.1029/2003GB002199.
- Krinner, G., N. Viovy, N. de Noblet-Ducoudré, J. Ogee, J. Polcher, P. Friedlingstein, P. Ciais, S. Sitch, and I. Prentice (2005b), A dynamic global vegetation model for studies of the coupled atmosphere-biosphere system, *Glob. Biogeochem. Cycles Biochem.*, 19(GB1012), doi:10.1029/2003GB002199.
- Laio, F., A. Porporato, L. Ridol, and I. Rodriguez-iturbe (2001), Plants in water-controlled ecosystems : active role in hydrologic processes and response to water stress II . Probabilistic soil moisture dynamics, *Adv. Water Resour.*, 24(7), 707–723.
- Li, D., M. Pan, Z. Cong, L. Zhang, and E. Wood (2013), Vegetation control on water and energy balance within the Budyko framework, *Water Resour. Res.*, 49(2), 969–976, doi:10.1002/wrcr.20107.
- Loik, M. E., D. D. Breshears, W. K. Lauenroth, and J. Belnap (2004), A multi-scale perspective of water pulses in dryland ecosystems: climatology and ecohydrology of the western USA., *Oecologia*, 141(2), 269–281, doi:10.1007/s00442-004-1570-y.

- Manoli, G., S. Bonetti, J.-C. Domec, M. Putti, G. Katul, and M. Marani (2014), Tree root systems competing for soil moisture in a 3D soil-plant model, *Adv. Water Resour.*, 66, 32–42, doi:10.1016/j.advwatres.2014.01.006.
- Markewitz, D., S. Devine, E. A Davidson, P. Brando, and D. C. Nepstad (2010), Soil moisture depletion under simulated drought in the Amazon: impacts on deep root uptake., *New Phytol.*, 187(3), 592–607, doi:10.1111/j.1469-8137.2010.03391.x.
- McDowell, N. et al. (2013), Evaluating theories of drought induced vegetation mortality using a multimodel–experiment framework, *New Phytol.*, 200(2), 304–321, doi:10.1111/nph.12465.
- McManus, J. F. (1999), A 0.5-million-year record of millennial-scale climate variability in the North Atlantic, *Science*, 283(5404), 971–975, doi:10.1126/science.283.5404.971.
- Medvigy, D., and C. Beaulieu (2012), Trends in Daily Solar Radiation and Precipitation Coefficients of Variation since 1984, *J. Clim.*, 25(4), 1330–1339, doi:10.1175/2011JCLI4115.1.
- Medvigy, D., S. C. Wofsy, J. W. Munger, and P. R. Moorcroft (2010), Responses of terrestrial ecosystems and carbon budgets to current and future environmental variability., *Proc. Natl. Acad. Sci. U. S. A.*, 107(18), 8275–80, doi:10.1073/pnas.0912032107.
- Mendel, M., S. Hergarten, and H. J. Neugebauer (2002), On a better understanding of hydraulic lift: A numerical study, *Water Resour. Res.*, 38(10), doi:10.1029/2001WR000911.
- Molini, A., G. G. Katul, and A. Porporato (2009), Revisiting rainfall clustering and intermittency across different climatic regimes, *Water Resour. Res.*, 45(11), W11403, doi:10.1029/2008WR007352.
- Moorcroft, P. R. (2006), How close are we to a predictive science of the biosphere?, *Trends Ecol. Evol.*, 21(7), 400–407, doi:10.1016/j.tree.2006.04.009.
- Myneni, R. B. et al. (2007), Large seasonal swings in leaf area of Amazon rainforests., *Proc. Natl. Acad. Sci. U. S. A.*, 104(12), 4820–4823, doi:10.1073/pnas.0611338104.
- Nagler, P. L., E. P. Glenn, H. Kim, W. Emmerich, R. L. Scott, T. E. Huxman, and a. R. Huete (2007), Relationship between evapotranspiration and precipitation pulses in a semiarid rangeland estimated by moisture flux towers and MODIS vegetation indices, *J. Arid Environ.*, 70(3), 443–462, doi:10.1016/j.jaridenv.2006.12.026.
- Nakai, T., G. Katul, A. Kotani, Y. Igarashi, T. Ohta, M. Suzuki, and T. Kumagai (2014), Radiative and precipitation controls on root zone soil moisture spectra, *Geophys. Reseach Lett.*, 41(21), 7546–7554, doi:10.1002/2014GL061745.
- Nepstad, D., C. de Carvalho, E. Davidson, P. Jipp, P. Lefebvre, G. Negreiros, E. da Silva, T. Stone, S. E. Trumbore, and S. Vieira (1994), The role of deep roots in the hydrological and carbon cycles of Amazonian forests and pastures, *Nature*, 372, 666–669, doi:10.1038/372666a0.
- Neumann, R., and Z. Cardon (2012), The magnitude of hydraulic redistribution by plant roots: a review and synthesis of empirical and modeling studies, *New Phytol.*, 194, 337–352.

- Norris, J. R., and M. Wild (2007), Trends in aerosol radiative effects over Europe inferred from observed cloud cover, solar “dimming,” and solar “brightening,” *J. Geophys. Res.*, *112*(D8), D08214, doi:10.1029/2006JD007794.
- Noy-Meir, I. (1973), Desert ecosystems: environment and producers, *Annu. Rev. Ecol. Syst.*, *4*(1973), 25–51.
- O’Gorman, P., and T. Schneider (2009), The physical basis for increases in precipitation extremes in simulations of 21st-century climate change, *Proc. Natl. Acad. Sci. U. S. A.*, *106*(35), 14773–14777, doi:10.1073/pnas.0907610106.
- Oishi, A. C., R. Oren, K. A. Novick, S. Palmroth, and G. G. Katul (2010), Interannual invariability of forest evapotranspiration and its consequence to water flow downstream, *Ecosystems*, *13*(3), 421–436, doi:10.1007/s10021-010-9328-3.
- Oleson, K. W. et al. (2013), *Technical Description of version 4.5 of the Community Land Model (CLM)*, Boulder, CO.
- Oliveira, R. S., T. E. Dawson, S. S. O. Burgess, and D. C. Nepstad (2005), Hydraulic redistribution in three Amazonian trees., *Oecologia*, *145*(3), 354–63, doi:10.1007/s00442-005-0108-2.
- Oren, R. et al. (2001), Soil fertility limits carbon sequestration by forest ecosystems in a CO₂ -enriched atmosphere, *Nature*, *411*, 469–472, doi:10.1038/35078064.
- Palmroth, S., C. A. Maier, H. R. McCarthy, A. C. Oishi, H.-S. Kim, K. H. Johnsen, G. G. Katul, and R. Oren (2005), Contrasting responses to drought of forest floor CO₂ efflux in a Loblolly pine plantation and a nearby Oak-Hickory forest, *Glob. Chang. Biol.*, *11*(3), 421–434, doi:10.1111/j.1365-2486.2005.00915.x.
- Palmroth, S., G. G. Katul, C. A. Maier, E. Ward, S. Manzoni, and G. Vico (2013), On the complementary relationship between marginal nitrogen and water-use efficiencies among *Pinus taeda* leaves grown under ambient and CO₂-enriched environments., *Ann. Bot.*, *111*(3), 467–77, doi:10.1093/aob/mcs268.
- Papalexiou, S. M., D. Koutsoyiannis, and C. Makropoulos (2013), How extreme is extreme? An assessment of daily rainfall distribution tails, *Hydrol. Earth Syst. Sci.*, *17*, 851–862, doi:10.5194/hess-17-851-2013.
- Pappas, C., S. Fatichi, S. Leuzinger, A. Wolf, and P. Burlando (2013), Sensitivity analysis of a process-based ecosystem model: Pinpointing parameterization and structural issues, *J. Geophys. Res. Biogeosciences*, *118*(2), 505–528, doi:10.1002/jgrg.20035.
- Pappas, C., S. Fatichi, S. Rimkus, P. Burlando, and M. O. Huber (2015), The role of local scale heterogeneities in terrestrial ecosystem modeling, *J. Geophys. Res. Biogeosciences*, *120*(2), doi:10.1002/2014JG002735.
- Paschalis, A. (2013), Modelling the space time structure of precipitation and its impact on basin response, ETH Zurich, Diss no. 21112.

- Paschalis, A., P. Molnar, S. Fatichi, and P. Burlando (2013), A stochastic model for high resolution space-time precipitation simulation, *Water Resour. Res.*, 49(12), 8400–8417, doi:10.1002/2013WR014437.
- Paschalis, A., P. Molnar, S. Fatichi, and P. Burlando (2014a), On temporal stochastic modeling of precipitation, nesting models across scales, *Adv. Water Resour.*, 63, 152–166, doi:10.1016/j.advwatres.2013.11.006.
- Paschalis, A., S. Fatichi, P. Molnar, S. Rimkus, and P. Burlando (2014b), On the effects of small scale space–time variability of rainfall on basin flood response, *J. Hydrol.*, 514, 313–327, doi:10.1016/j.jhydrol.2014.04.014.
- Peng, S. et al. (2013), Asymmetric effects of daytime and night-time warming on Northern Hemisphere vegetation., *Nature*, 501(7465), 88–92, doi:10.1038/nature12434.
- Peters, D. (2000), Climatic variation and simulated patterns in seedling establishment of two dominant grasses at a semi-arid arid-grassland ecotone, *J. Veg. Sci.*, 44(4), 493–504, doi:10.2307/3246579.
- Porporato, A., E. Daly, and I. Rodriguez-Iturbe (2004), Soil water balance and ecosystem response to climate change, *Am. Nat.*, 164(5), 625–632, doi:10.1086/424970.
- Pregitzer, K., R. Hendrick, and R. Fogel (1993), The demography of fine roots in response to patches of water and nitrogen, *New Phytol.*, 125(3), 575–580.
- Press, W., S. Teukolsky, W. Vetterling, and B. Flanner (1992), *Numerical recipes*, Cambridge University Press.
- Pritchard, S. G., A. E. Strand, M. L. McCormack, M. A. Davis, A. C. Finzi, R. B. Jackson, R. Matamala, H. H. Rogers, and R. Oren (2008), Fine root dynamics in a loblolly pine forest are influenced by free-air-CO₂ -enrichment: a six-year-minirhizotron study, *Glob. Chang. Biol.*, 14(3), 588–602, doi:10.1111/j.1365-2486.2007.01523.x.
- Pumpanen, J., H. Ilvesniemi, M. Perämäki, and P. Hari (2003), Seasonal patterns of soil CO₂ efflux and soil air CO₂ concentration in a Scots pine forest: comparison of two chamber techniques, *Glob. Chang. Biol.*, 9(3), 371–382.
- Reichmann, L., O. Sala, and D. Peters (2013), Precipitation legacies in desert grassland primary production occur through previous-year tiller density, *Ecology*, 94(2), 435–443, doi:10.1890/12-1237.1.
- Reichstein, M. et al. (2013), Climate extremes and the carbon cycle., *Nature*, 500(7462), 287–95, doi:10.1038/nature12350.
- Renard, K. G., M. H. Nichols, D. A. Woolhiser, and H. B. Osborn (2008), A brief background on the U.S. Department of Agriculture Agricultural Research Service Walnut Gulch Experimental Watershed, *Water Resour. Res.*, 44(5), doi:10.1029/2006WR005691.

- Restrepo-Coupe, N. et al. (2013), What drives the seasonality of photosynthesis across the Amazon basin? A cross-site analysis of eddy flux tower measurements from the Brasil flux network, *Agric. For. Meteorol.*, 182-183, 128–144, doi:10.1016/j.agrformet.2013.04.031.
- Ridolfi, L., P. D’Odorico, A. Porporato, and I. Rodriguez-Iturbe (2000), Impact of climate variability on the vegetation water stress, *J. Geophys. Res. Atmos.*, 105(D14), 13–18, doi:10.1029/2000JD900206.
- Rigby, J. R., and A. Porporato (2008), Spring frost risk in a changing climate, *Geophys. Res. Lett.*, 35(12), doi:10.1029/2008GL033955.
- Ritchie, J. C., M. A. Nearing, M. H. Nichols, and C. A. Ritchie (2005), Patterns of soil erosion and redeposition on Lucky Hills watershed, Walnut Gulch Experimental Watershed, Arizona, *Catena*, 61(2-3), 122–130, doi:10.1016/j.catena.2005.03.012.
- Rodriguez-Iturbe, I., A. Porporato, F. Laio, and L. Ridol (2001), Plants in water-controlled ecosystems : active role in hydrologic processes and response to water stress I . Scope and general outline, *Adv. Water Resour.*, 24(7), 695–705.
- Saleska, S. et al. (2003), Carbon in Amazon forests: unexpected seasonal fluxes and disturbance-induced losses, *Science*, 302(5650), 1554–1558.
- Saleska, S. R., K. Didan, A. R. Huete, and H. R. da Rocha (2007), Amazon forests green-up during 2005 drought, *Science*, 318(5850), 612, doi:10.1126/science.1146663.
- Scott, R., W. Shuttleworth, T. O. Keefer, and A. Warrick (2000), Modeling multiyear observations of soil moisture recharge in the semiarid American Southwest, *Water Resour. Res.*, 36(8), 2233–2247.
- Sellers, P., D. Randall, and G. Collatz (1996), A revised land surface parameterization (SiB2) for atmospheric GCMs. Part I: Model formulation, *J. Clim.*, 9, 676–705.
- Siqueira, M., G. G. Katul, and A. Porporato (2009), Soil Moisture Feedbacks on Convection Triggers: The Role of Soil–Plant Hydrodynamics, *J. Hydrometeorol.*, 10(1), 96–112, doi:10.1175/2008JHM1027.1.
- Sitch, S. et al. (2003), Evaluation of ecosystem dynamics, plant geography and terrestrial carbon cycling in the LPJ dynamic global vegetation model, *Glob. Chang. Biol.*, 9(2), 161–185, doi:10.1046/j.1365-2486.2003.00569.x.
- Sitch, S. et al. (2008), Evaluation of the terrestrial carbon cycle, future plant geography and climate-carbon cycle feedbacks using five Dynamic Global Vegetation Models (DGVMs), *Glob. Chang. Biol.*, 14(9), 2015–2039, doi:10.1111/j.1365-2486.2008.01626.x.
- Smith, N. et al. (2014), Toward a better integration of biological data from precipitation manipulation experiments into Earth system models, *Rev. Geophys.*, 52(3), 412–434, doi:10.1002/2014RG000458.Received.
- Stoy, P. C., G. G. Katul, M. B. S. Siqueira, J.-Y. Juang, K. A. Novick, H. R. McCarthy, A. Christopher Oishi, J. M. Uebelherr, H.-S. Kim, and R. Oren (2006), Separating the effects of climate and

- vegetation on evapotranspiration along a successional chronosequence in the southeastern US, *Glob. Chang. Biol.*, 12(11), 2115–2135, doi:10.1111/j.1365-2486.2006.01244.x.
- Stoy, P. C., S. Palmroth, A. C. Oishi, M. B. S. Siqueira, J.-Y. Juang, K. A. Novick, E. J. Ward, G. G. Katul, and R. Oren (2007), Are ecosystem carbon inputs and outputs coupled at short time scales? A case study from adjacent pine and hardwood forests using impulse-response analysis., *Plant. Cell Environ.*, 30(6), doi:10.1111/j.1365-3040.2007.01655.x.
- Stoy, P. C. et al. (2013), Evaluating the agreement between measurements and models of net ecosystem exchange at different times and timescales using wavelet coherence: an example using data from the North American Carbon Program Site-Level Interim Synthesis, *Biogeosciences*, 10(11), 6893–6909, doi:10.5194/bg-10-6893-2013.
- Sun, F., M. L. Roderick, and G. D. Farquhar (2012), Changes in the variability of global land precipitation, *Geophys. Res. Lett.*, 39(19), doi:10.1029/2012GL053369.
- Sun, Y., S. Solomon, A. Dai, and R. W. Portmann (2007), How Often Will It Rain?, *J. Clim.*, 20(19), 4801–4818, doi:10.1175/JCLI4263.1.
- Suni, T., J. Rinne, A. Reissell, N. Altimir, P. Keronen, U. Rannik, M. Dal Maso, M. Kulmala, and T. Vesala (2003), Long-term measurements of surface fluxes above a Scots pine forest in Hyytiälä, southern Finland, 1996-2001, *Boreal Environ. Res.*, 8, 287–301.
- Swemmer, A. M., A. K. Knapp, and H. A. Snyman (2007), Intra-seasonal precipitation patterns and above-ground productivity in three perennial grasslands, *J. Ecol.*, 95(4), 780–788, doi:10.1111/j.1365-2745.2007.01237.x.
- Thornton, P. K., P. J. Ericksen, M. Herrero, and A. J. Challinor (2014), Climate variability and vulnerability to climate change: a review., *Glob. Chang. Biol.*, 20(11), 3313–3328, doi:10.1111/gcb.12581.
- Tian, H., J. M. Melillo, D. W. Kicklighter, A. McGuire, J. Helfrich III, B. Moore III, and C. Vorosmarty (1998), Effect of interannual climate variability on carbon storage in Amazonian ecosystems, *Nature*, 396, 664–667.
- Todd-Brown, K. E. O. et al. (2014), Changes in soil organic carbon storage predicted by Earth system models during the 21st century, *Biogeosciences*, 11(8), 2341–2356, doi:10.5194/bg-11-2341-2014.
- Torrence, C., and G. Compo (1998), A practical guide to wavelet analysis, *Bull. Am. Meteorol. Soc.*, 79(1), 61–78.
- Vargas, R., M. S. Carbone, M. Reichstein, and D. D. Baldocchi (2010), Frontiers and challenges in soil respiration research: from measurements to model-data integration, *Biogeochemistry*, 102(1-3), 1–13, doi:10.1007/s10533-010-9462-1.
- Vico, G. et al. (2014), Climatic, ecophysiological, and phenological controls on plant ecohydrological strategies in seasonally dry ecosystems, *Ecohydrology*, *In Press*, doi:10.1002/eco.1533.

- Vinnikov, K. Y. (2002), Diurnal and seasonal cycles of trends of surface air temperature, *J. Geophys. Res.*, 107(D22), 4641, doi:10.1029/2001JD002007.
- Volpe, V., M. Marani, J. D. Albertson, and G. Katul (2013), Root controls on water redistribution and carbon uptake in the soil-plant system under current and future climate, *Adv. Water Resour.*, 60, 110–120, doi:10.1016/j.advwatres.2013.07.008.
- Wan, S., Y. Luo, and L. L. Wallace (2002), Changes in microclimate induced by experimental warming and clipping in tallgrass prairie, *Glob. Chang. Biol.*, 8(8), 754–768, doi:10.1046/j.1365-2486.2002.00510.x.
- Wild, M., H. Gilgen, A. Roesch, A. Ohmura, C. N. Long, E. G. Dutton, B. Forgan, A. Kallis, V. Russak, and A. Tsvetkov (2005), From dimming to brightening: decadal changes in solar radiation at Earth's surface., *Science*, 308(5723), 847–850, doi:10.1126/science.1103215.
- Williams, C. A., N. Hanan, R. J. Scholes, and W. Kutsch (2009), Complexity in water and carbon dioxide fluxes following rain pulses in an African savanna., *Oecologia*, 161(3), 469–80, doi:10.1007/s00442-009-1405-y.
- Wilson, K. et al. (2002), Energy balance closure at FLUXNET sites, *Agric. For. Meteorol.*, 113(1-4), 223–243, doi:10.1016/S0168-1923(02)00109-0.
- Wilson, K. B., and D. D. Baldocchi (2000), Seasonal and interannual variability of energy fluxes over a broadleaved temperate deciduous forest in North America, *Agric. For. Meteorol.*, 100(1), 1–18, doi:10.1016/S0168-1923(99)00088-X.
- Wohlfahrt, G., and L. Gu (2015), Opinion: The many meanings of gross photosynthesis and their implication for photosynthesis research from leaf to globe., *Plant. Cell Environ.*, *In Press*, doi:10.1111/pce.12569.
- Wu, Z., P. Dijkstra, G. W. Koch, J. Peñuelas, and B. A. Hungate (2011), Responses of terrestrial ecosystems to temperature and precipitation change: a meta-analysis of experimental manipulation, *Glob. Chang. Biol.*, 17(2), 927–942, doi:10.1111/j.1365-2486.2010.02302.x.
- Xia, J., J. Chen, S. Piao, P. Ciais, Y. Luo, and S. Wan (2014), Terrestrial carbon cycle affected by non-uniform climate warming, *Nat. Geosci.*, 7(3), 173–180, doi:10.1038/ngeo2093.
- Xu, C., N. G. McDowell, S. Sevanto, and R. A. Fisher (2013), Our limited ability to predict vegetation dynamics under water stress, *New Phytol.*, 200(2), 298–300.
- Yan, B., and R. Dickinson (2014), Modeling hydraulic redistribution and ecosystem response to droughts over the Amazon basin using Community Land Model 4.0 (CLM4), *J. Geophys. Res. Biogeosciences*, 119, 2130–2143, doi:10.1002/2014JG002694. Received.
- Yuan, W. et al. (2007), Deriving a light use efficiency model from eddy covariance flux data for predicting daily gross primary production across biomes, *Agric. For. Meteorol.*, 143(3-4), 189–207, doi:10.1016/j.agrformet.2006.12.001.

Yuan, Z. Y., and H. Chen (2010), Fine Root Biomass, Production, Turnover Rates, and Nutrient Contents in Boreal Forest Ecosystems in Relation to Species, Climate, Fertility, and Stand Age: Literature Review and Meta-Analyses, *CRC. Crit. Rev. Plant Sci.*, 29(4), 204–221, doi:10.1080/07352689.2010.483579.

Author Manuscript

List of Tables

Table 1: Summary of the meteorological input scenarios

Input Scenarios	
Combined cases	
1	<i>Control Scenario:</i> Observed Data
2	<i>Periodic Input:</i> All inputs preserve only the diurnal and seasonal variability of precipitation, temperature, and radiation
3	<i>Randomized Input:</i> Precipitation, temperature, and incoming radiation are simultaneously randomized by sampling without replacement, while preserving the seasonal and diurnal cycle and their conditional distributions
Precipitation	
4	<i>Randomized precip.:</i> Precipitation is randomized with sampling without replacement, while preserving the interannual, seasonal and diurnal cycles
5	<i>No IAV of precip.:</i> Interannual variability of precipitation is removed from the observed time series
6	<i>More peaky precip.:</i> Precipitation peaks are enhanced by employing a probability transform, while preserving the interannual variability of precipitation
7	<i>Less peaky precip.:</i> Peaks of precipitation are reduced by applying a moving average filter of 12 hours. The interannual variability, and approximately the distribution of depth per event is preserved
Temperature	
8	<i>Randomized temperature:</i> Temperature series are randomized with sampling without replacement, while preserving the interannual, seasonal, and diurnal cycles
9	<i>No IAV of temperature:</i> Interannual variability of temperature is removed from the observed time series
10	<i>Less extreme temperature:</i> A moving average filter of 12 hours is applied to the temperature time series
Radiation	
11	<i>Randomized radiation:</i> Radiation series are randomized with sampling without replacement, while preserving the interannual, seasonal, and diurnal cycles
12	<i>No IAV of radiation:</i> Interannual variability of radiation is removed from the observed time series

List of Figures

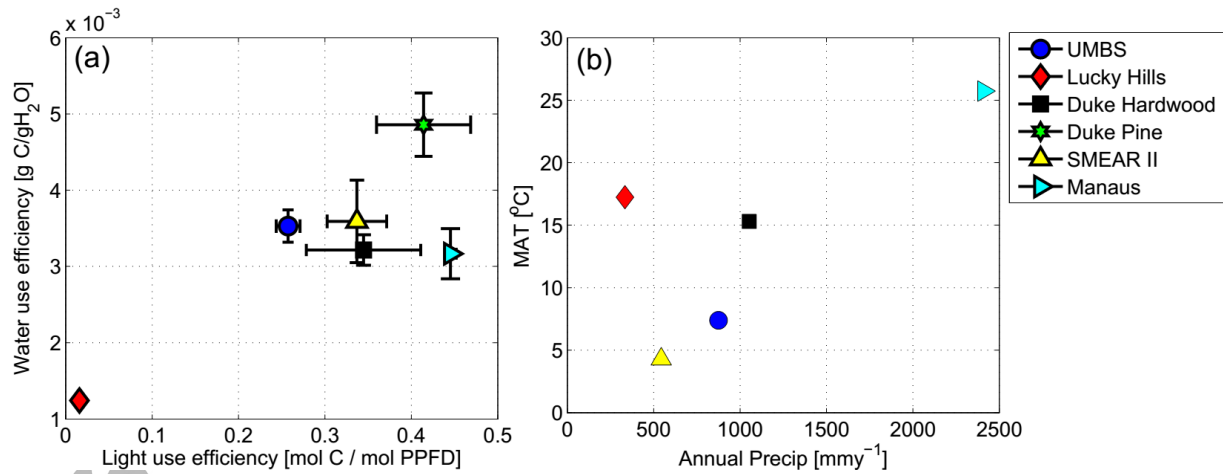


Figure 1: (a) Water use efficiency (*WUE*) and light use efficiency (*LUE*) defined as the ratios of annual *GPP* to annual transpiration and annual incoming photosynthetic active radiation, respectively, and (b) Mean annual precipitation and mean annual air temperature (MAT) for the analyzed stations. Errorbars correspond to the annual standard deviations.

Author Manuscript

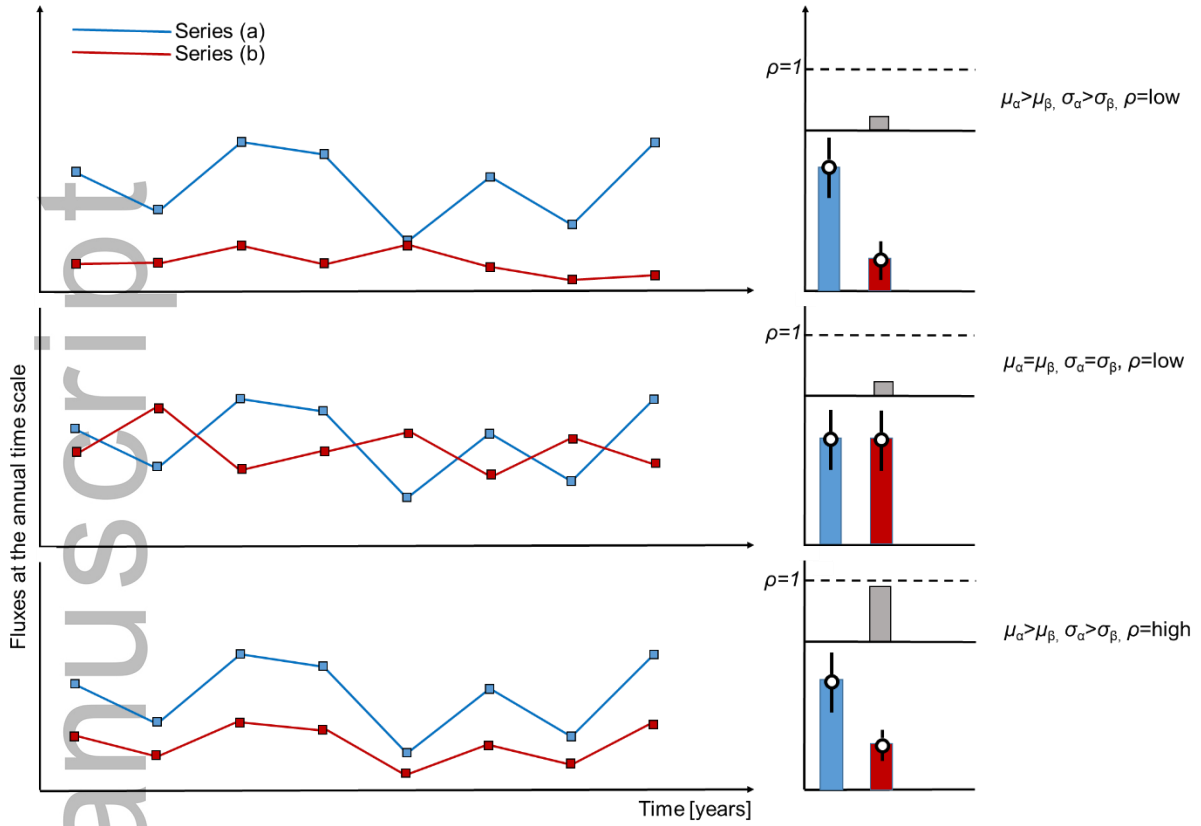


Figure 2: A schematic representation of the statistical evaluation presented in Figures 3-4: μ stands for mean value, σ is the standard deviation, and ρ is the correlation coefficient between series (a) and (b).

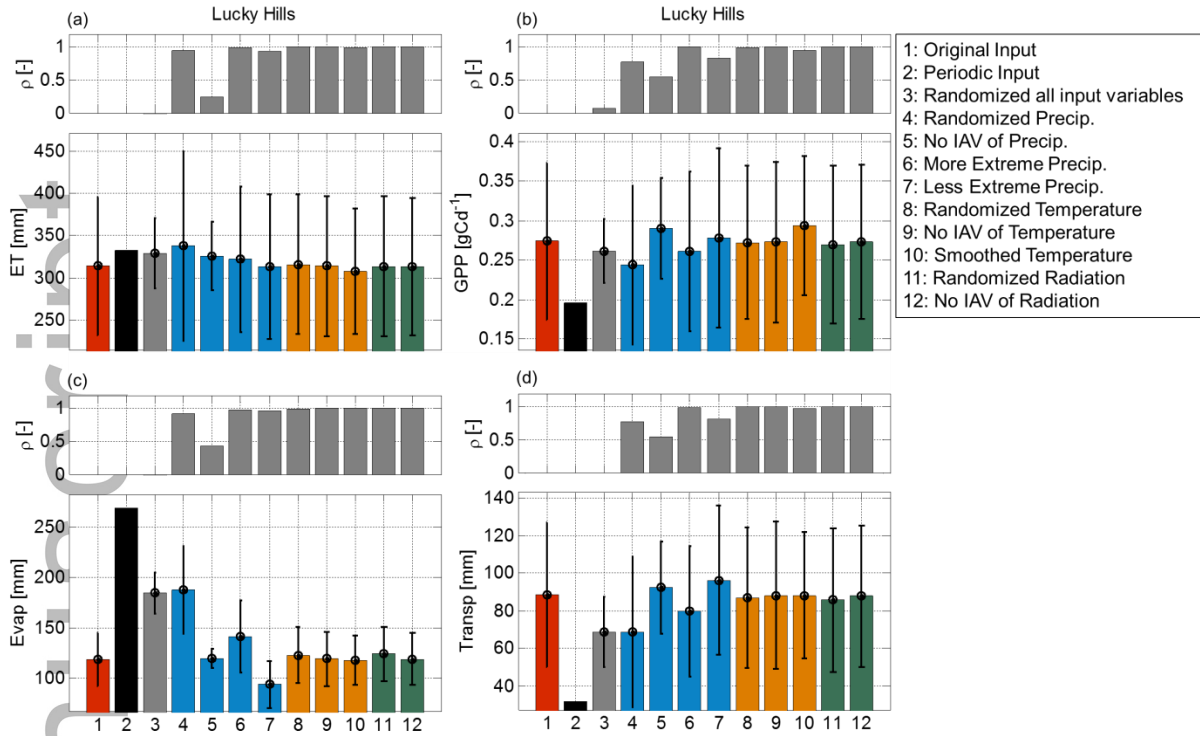


Figure 3: Interannual statistics for the Lucky Hills station for (a) Evapotranspiration, (b) Gross Primary Production of the evergreen shrubs (creosote bush), (c) Evaporation, and (d) Transpiration of the evergreen shrubs. The lower part of each panel shows the mean value (bars) and the standard deviation (errorbars) for the 12 different meteorological input scenarios. Input scenarios related to perturbing precipitation only are marked as blue, input scenarios related to perturbing temperature only are shown in yellow, and input scenarios related to perturbing radiation only are shown in green. The upper part of each panel shows the correlation coefficient between the output of each scenario for a given variable at the annual scale, and the output of the simulation of the control scenario (1). Correlation values $\rho[-]$ are shown for the cases (3-12). For case the 1, it is trivial that $\rho=1$.

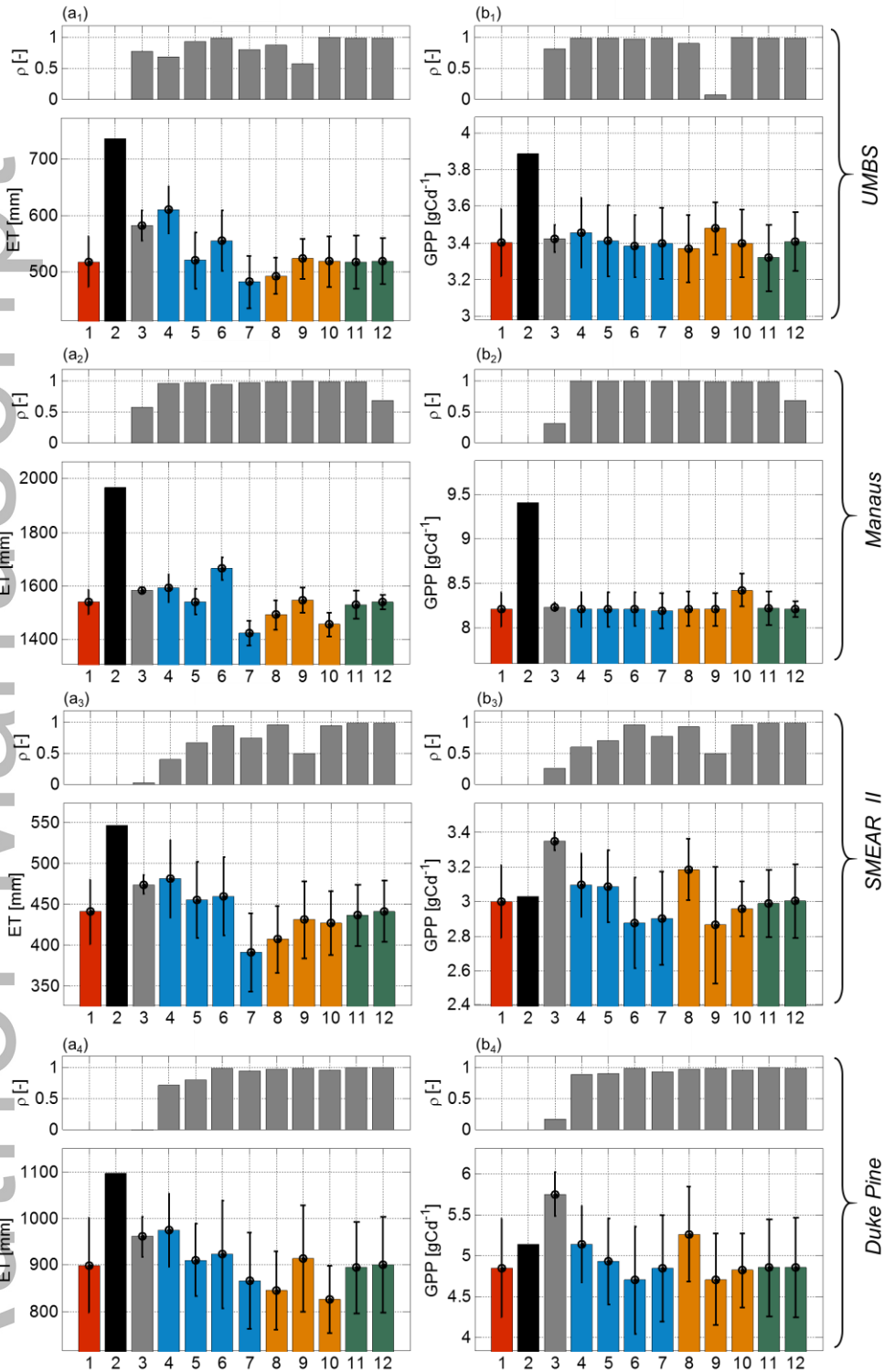


Figure 4: Same as Figure 3 but for the other sites. In this Figure only the panels of (a) Evapotranspiration, and (b) Gross Primary Production are shown. Subscripts 1-4 refer to the (1) UMBS, (2) Manaus, (3) SMEAR II, and (4) Duke Forest sites respectively.

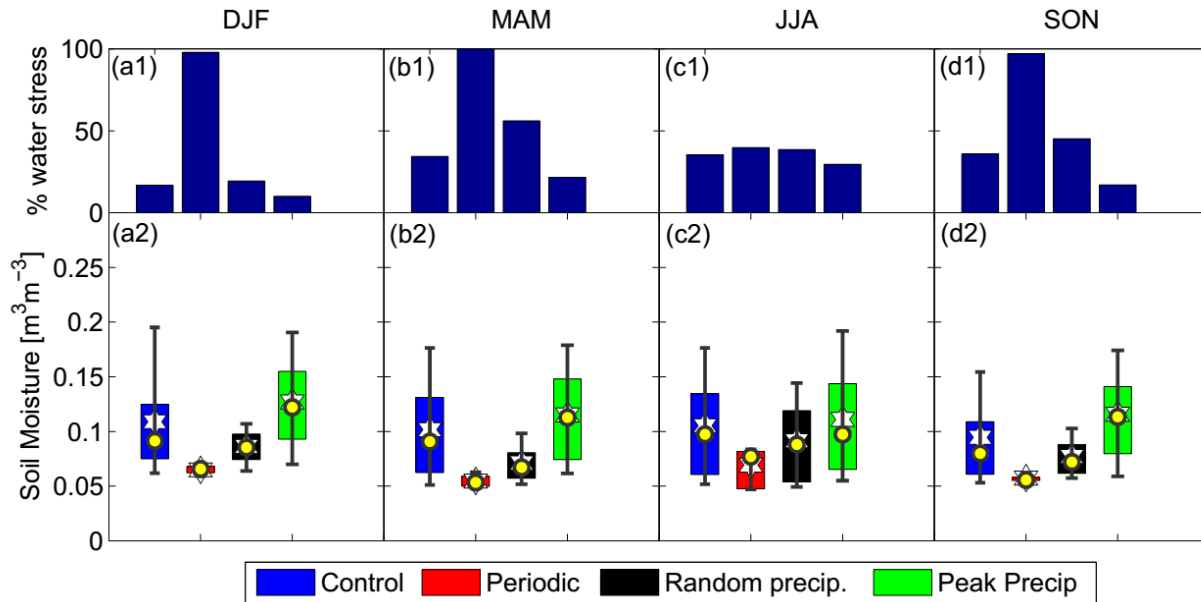


Figure 5: Analysis of the plant water stress for the Lucky Hills site (see section 4.2). The four panels represent the four seasons. The upper panels (a1, b1, c1, d1) show the percentage of time vegetation is under water stress for the four different precipitation input scenarios (cases 1-2-4-6 in Figure 3). The lower panels (a2, b2, c2, d2) show a boxplot of the soil moisture integrated in the root zone. Boxes represent the 25%-75% percentiles, bars the 10%-90% percentiles, circles show the mean value, and stars show the median value.

Author Manuscript

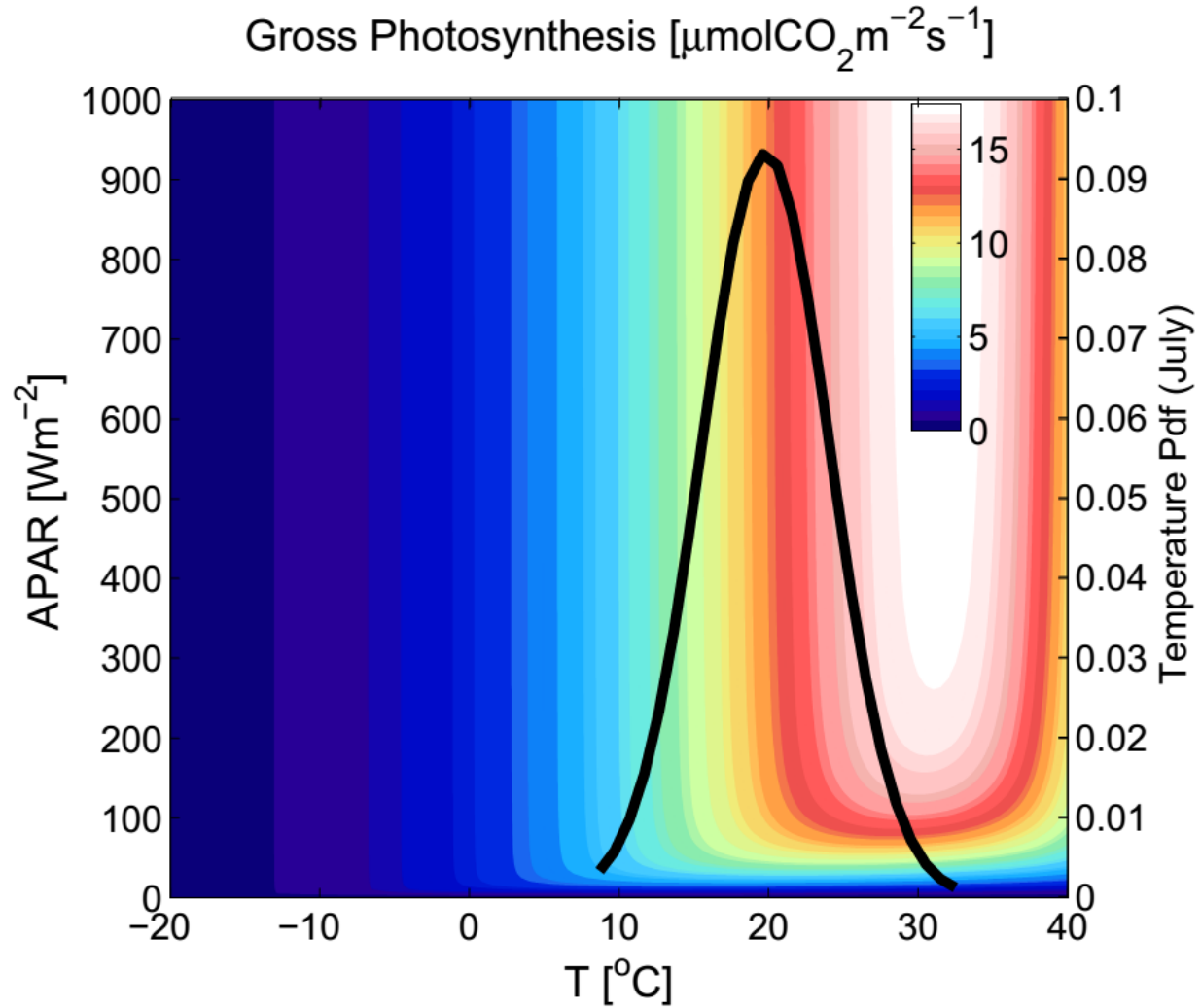


Figure 6: Response gross photosynthesis (A_g) to absorbed photosynthetic active radiation ($APAR$) and leaf temperature (T) as estimated by the model. The contours show A_g according to the colorbar. The photosynthesis biochemical parameters are the same as the parametrization of the PFT representing the deciduous forest in UMBS, and for this plot a relative humidity $U = 0.8$ and an atmospheric CO_2 concentration of 380 ppm were considered. The thick black line shows a normal fit of the probability density function of hourly air temperatures during July in UMBS (see section 4.3).

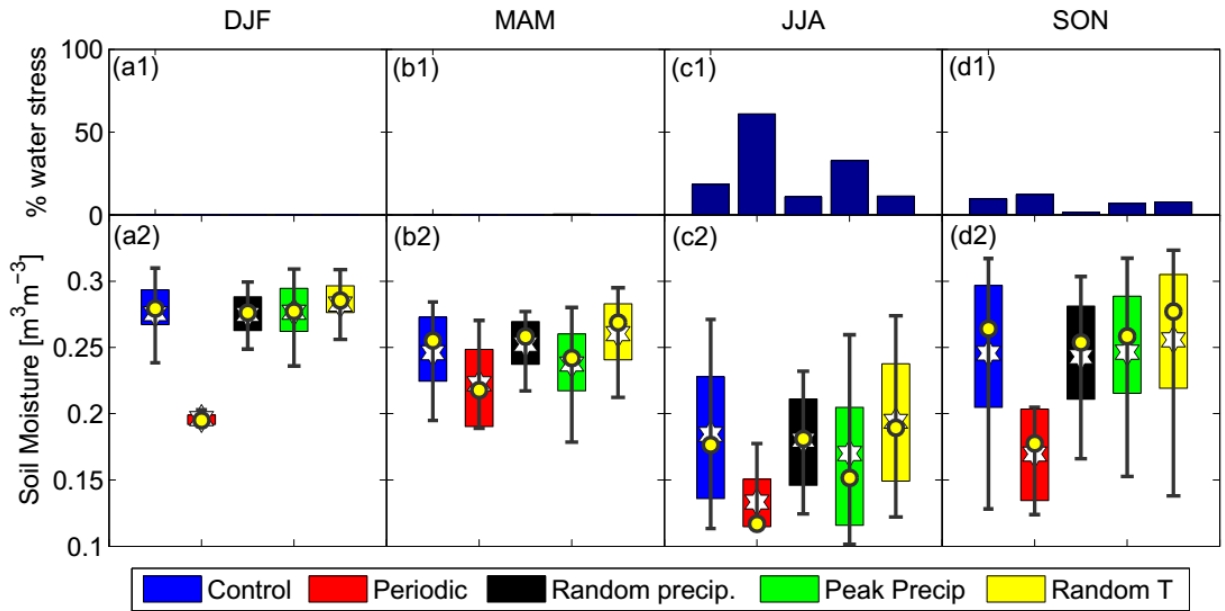


Figure 7: Same as Figure 5 but for the SMEAR II site (see section 4.5). The scenarios shown are the control scenario (blue, case 1), the scenario with periodic input (red, case 2), the scenario with randomized precipitation at the highest frequency (black, case 4), the scenario where precipitation peaks are enhanced (green, case 6), and the scenario where temperature is randomized at the higher frequency (yellow, case 8).

Author Manuscript

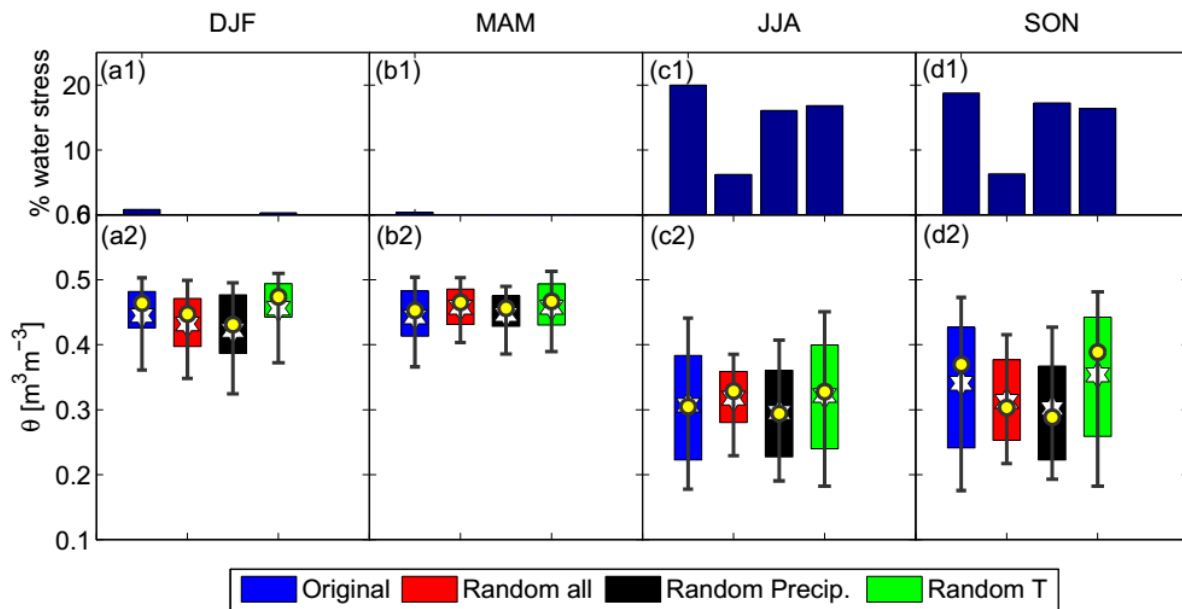


Figure 8: Same as Figure 5 but for the pine plantation in Duke forest (see section 4.6). The scenarios shown are the control scenario (blue, case 1), the scenario with randomized precipitation, temperature and radiation at the highest frequency (red, case 2), the scenario with randomized precipitation (black, case 4) and temperature (green, case 8) at the highest frequency.

Author Manuscript

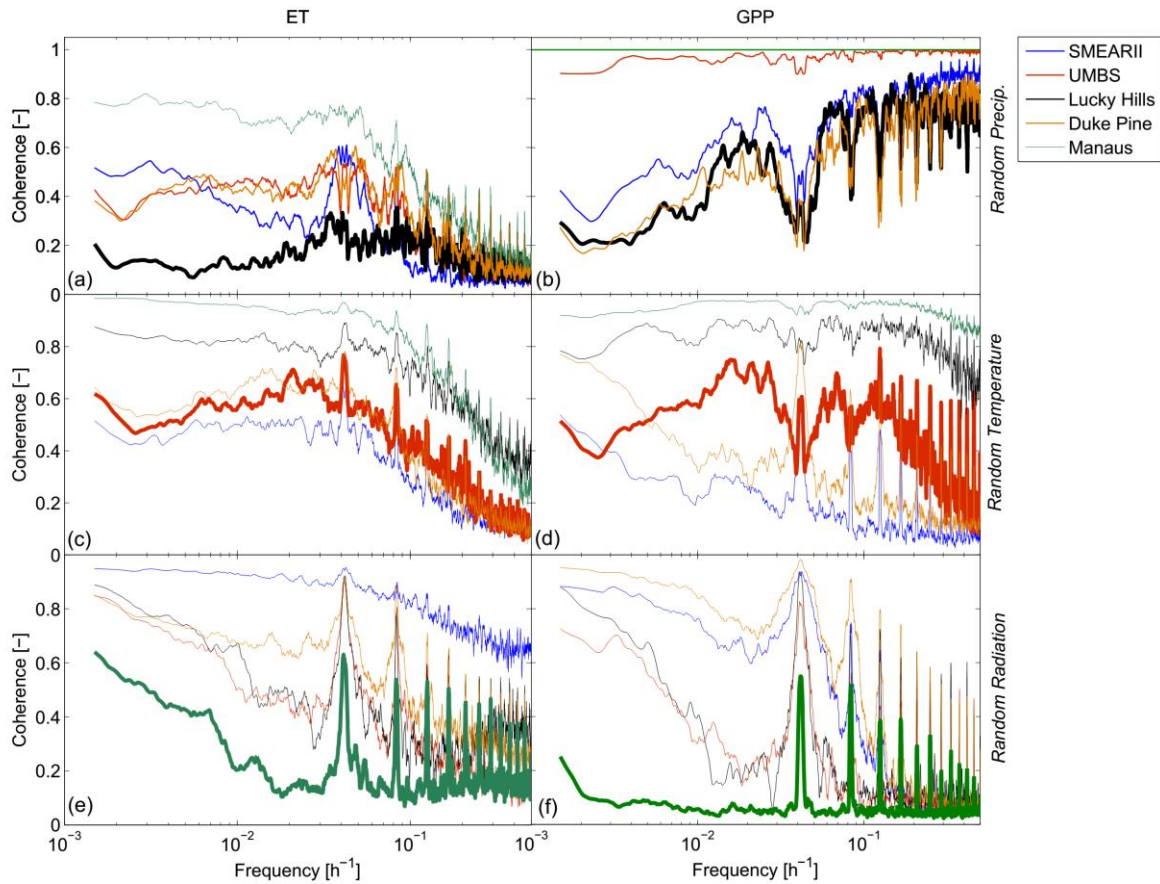


Figure 9: Squared coherence spectra between the simulated time series of *ET* (a, c, d) and *GPP* (b, d, f) between the control scenario and the synthetic input scenarios that randomize precipitation (a, b), temperature (c, d), and incoming radiation (e, f) at the highest frequency (1 h^{-1}). For each panel, the atmospheric variable of interest, which is the most important limiting factor for the ecosystem functioning is marked as a bold line.

Autho

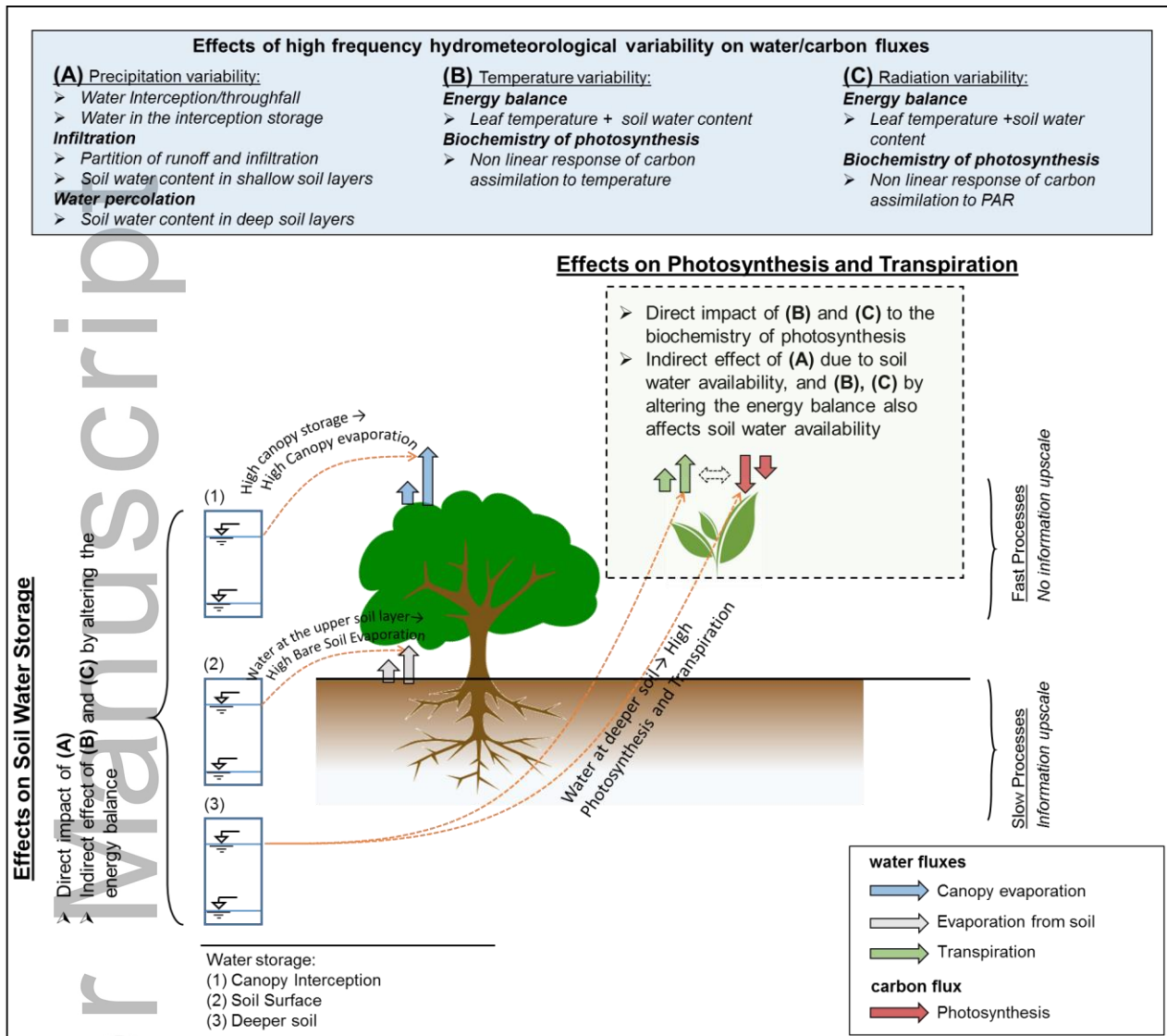
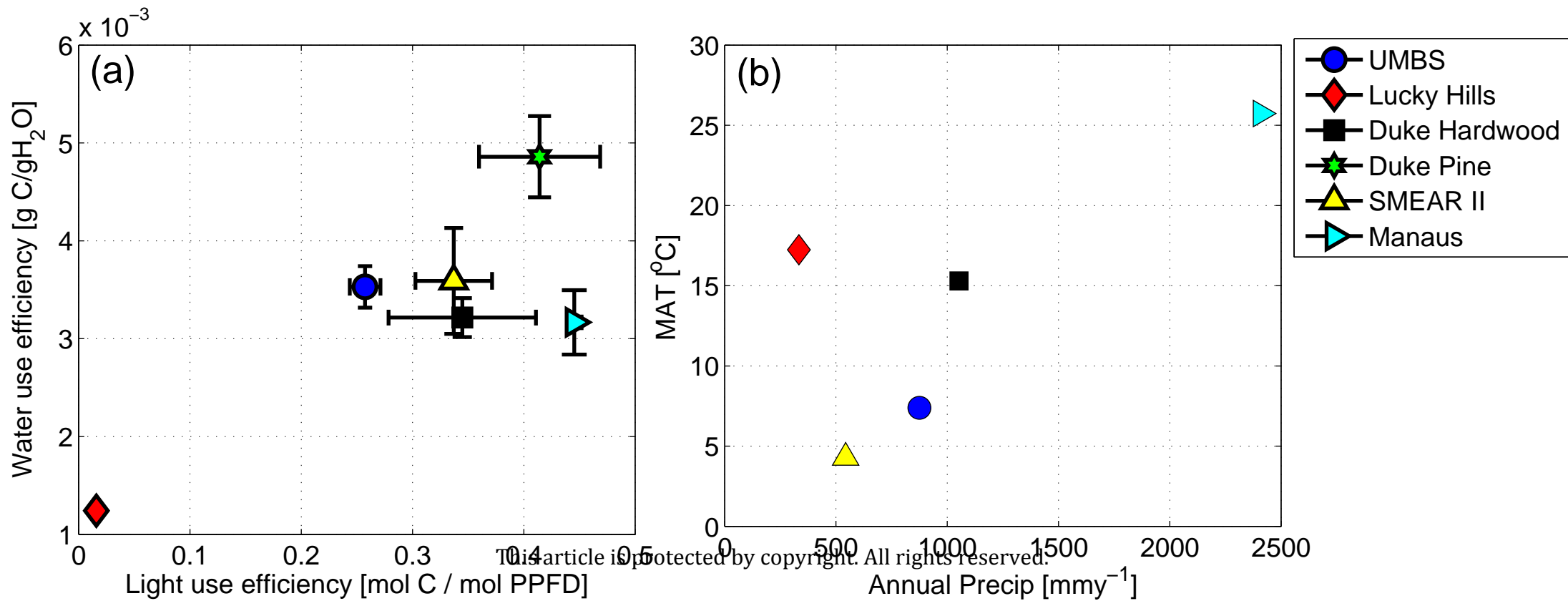
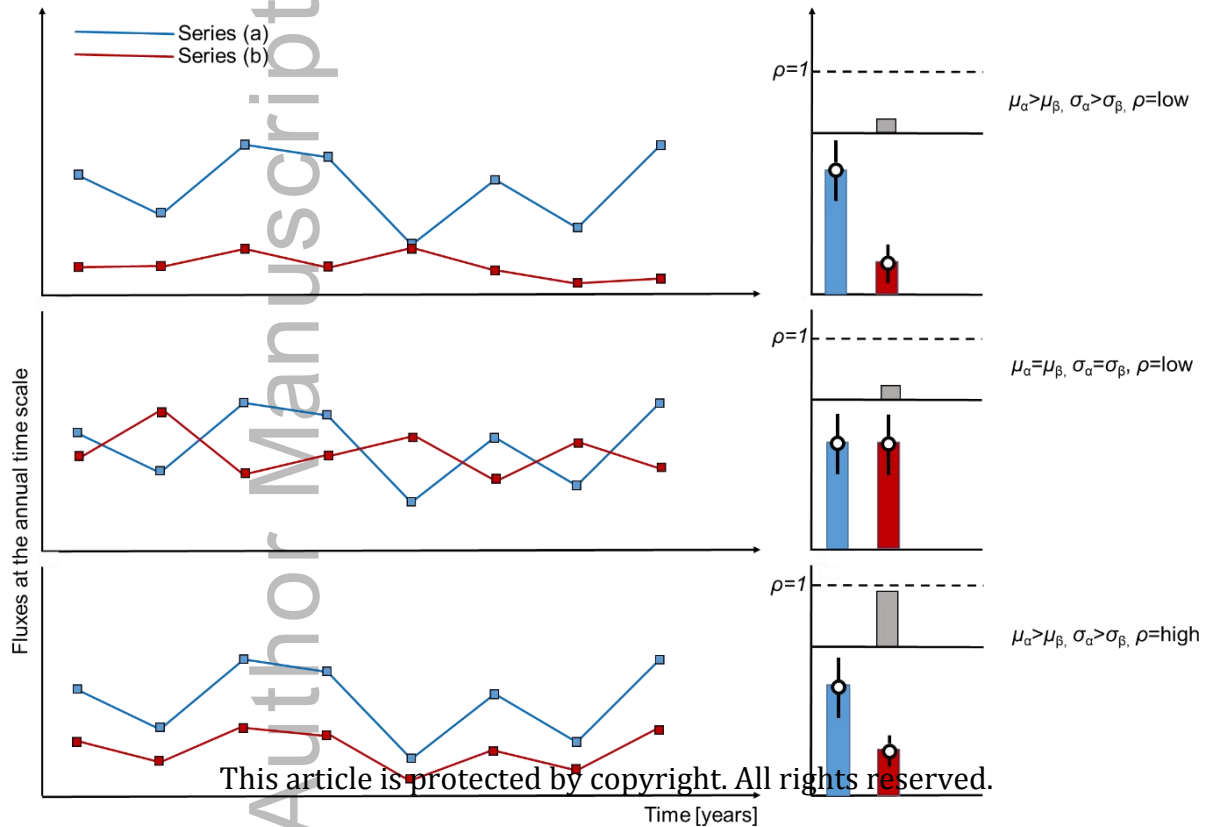
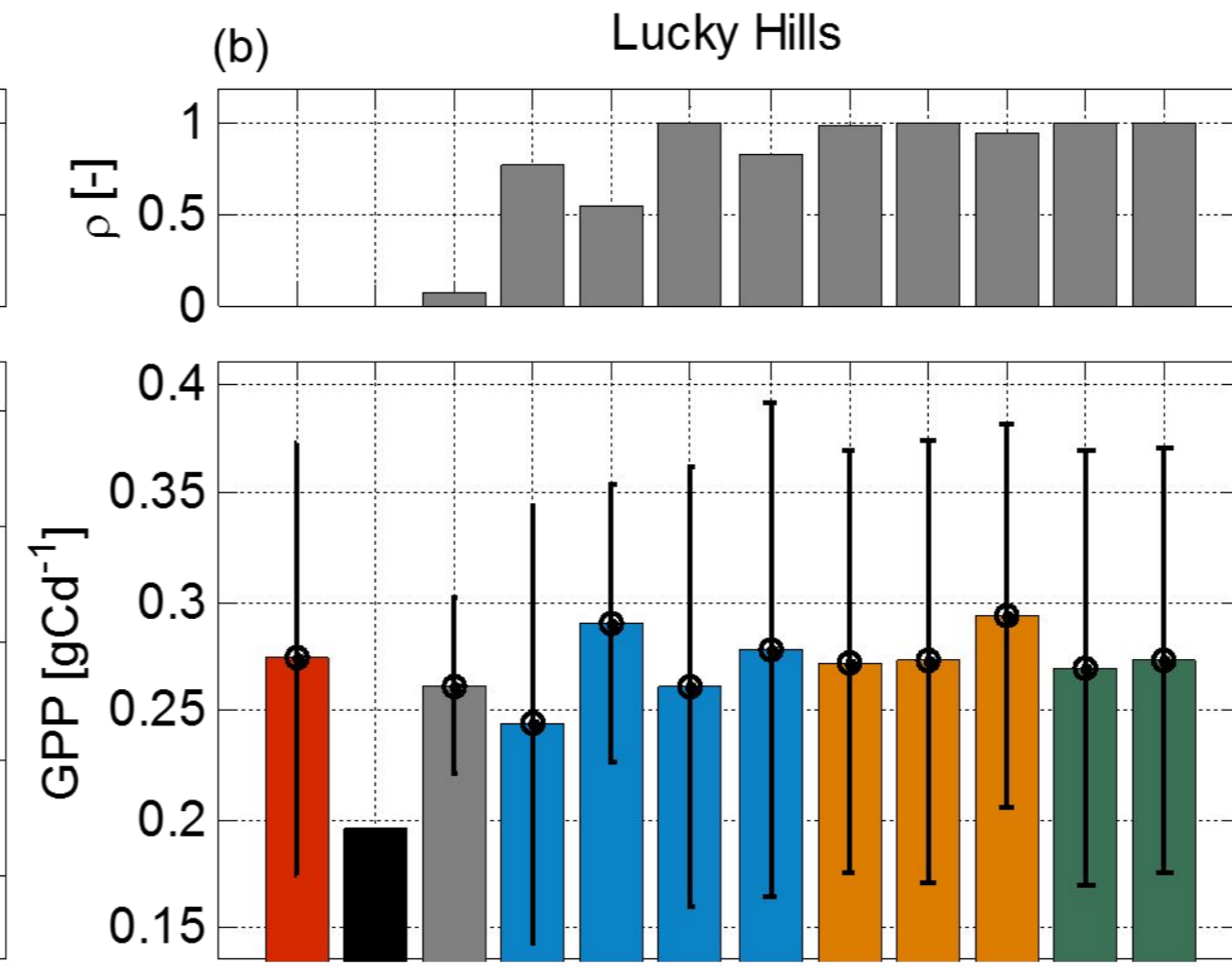
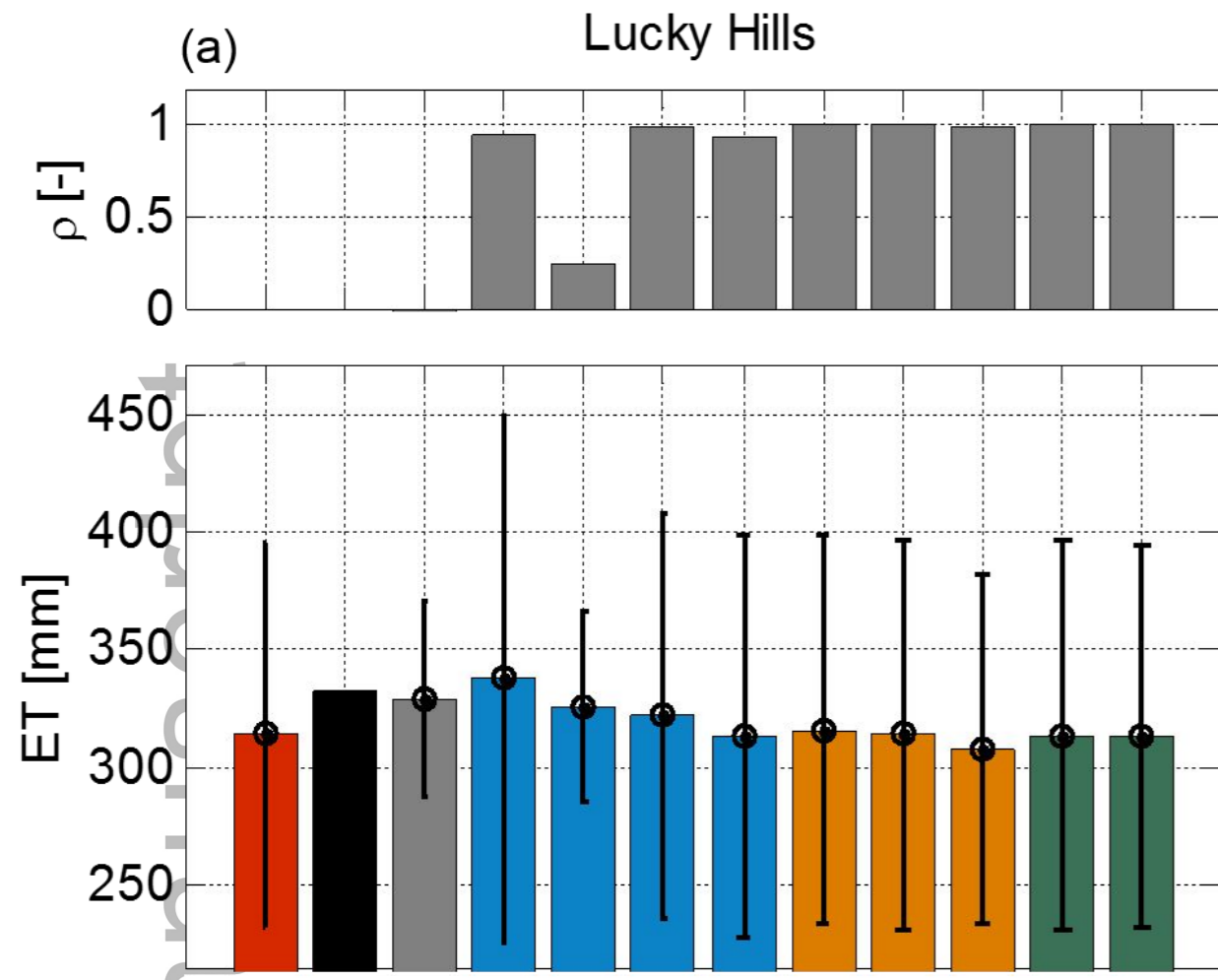


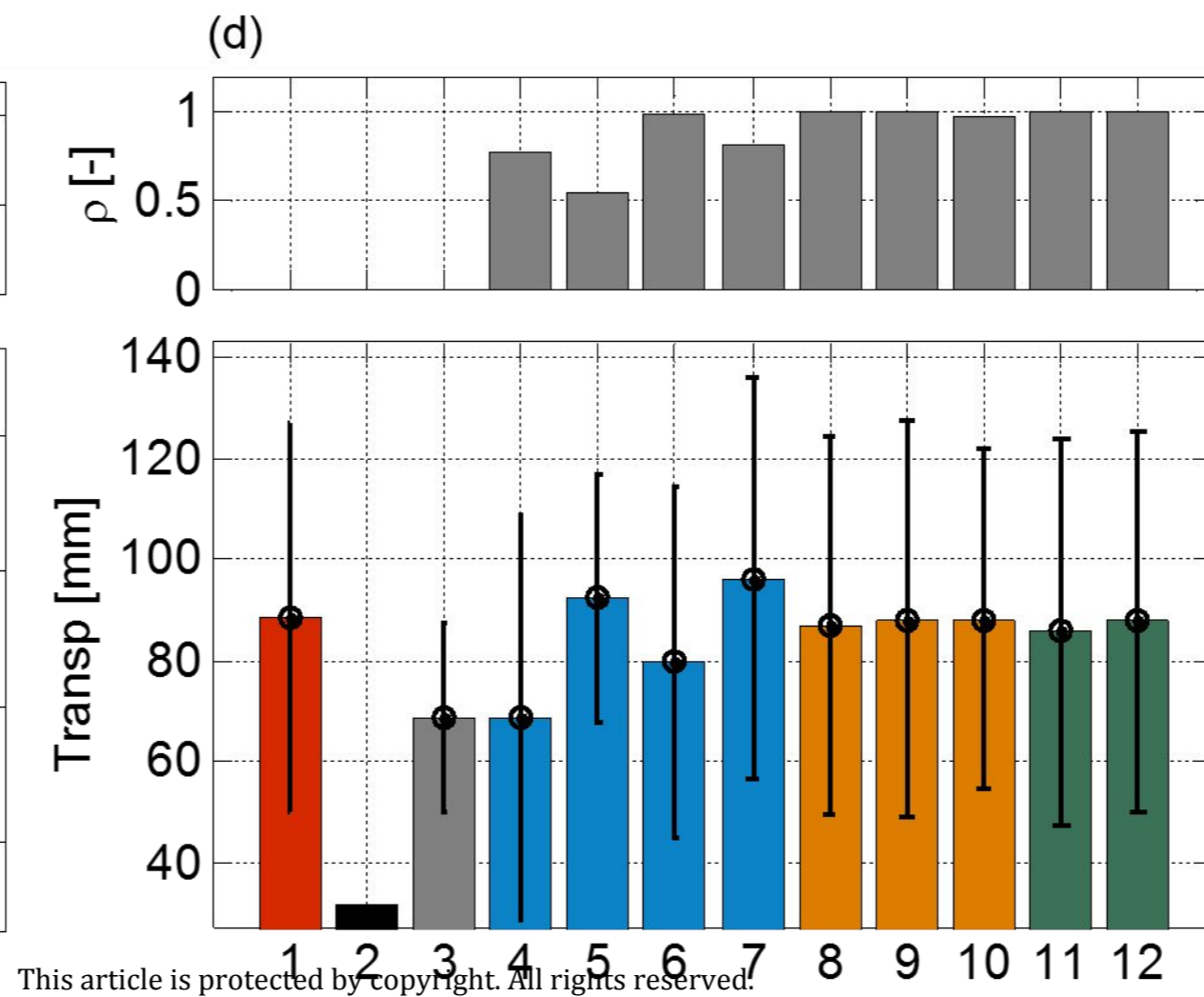
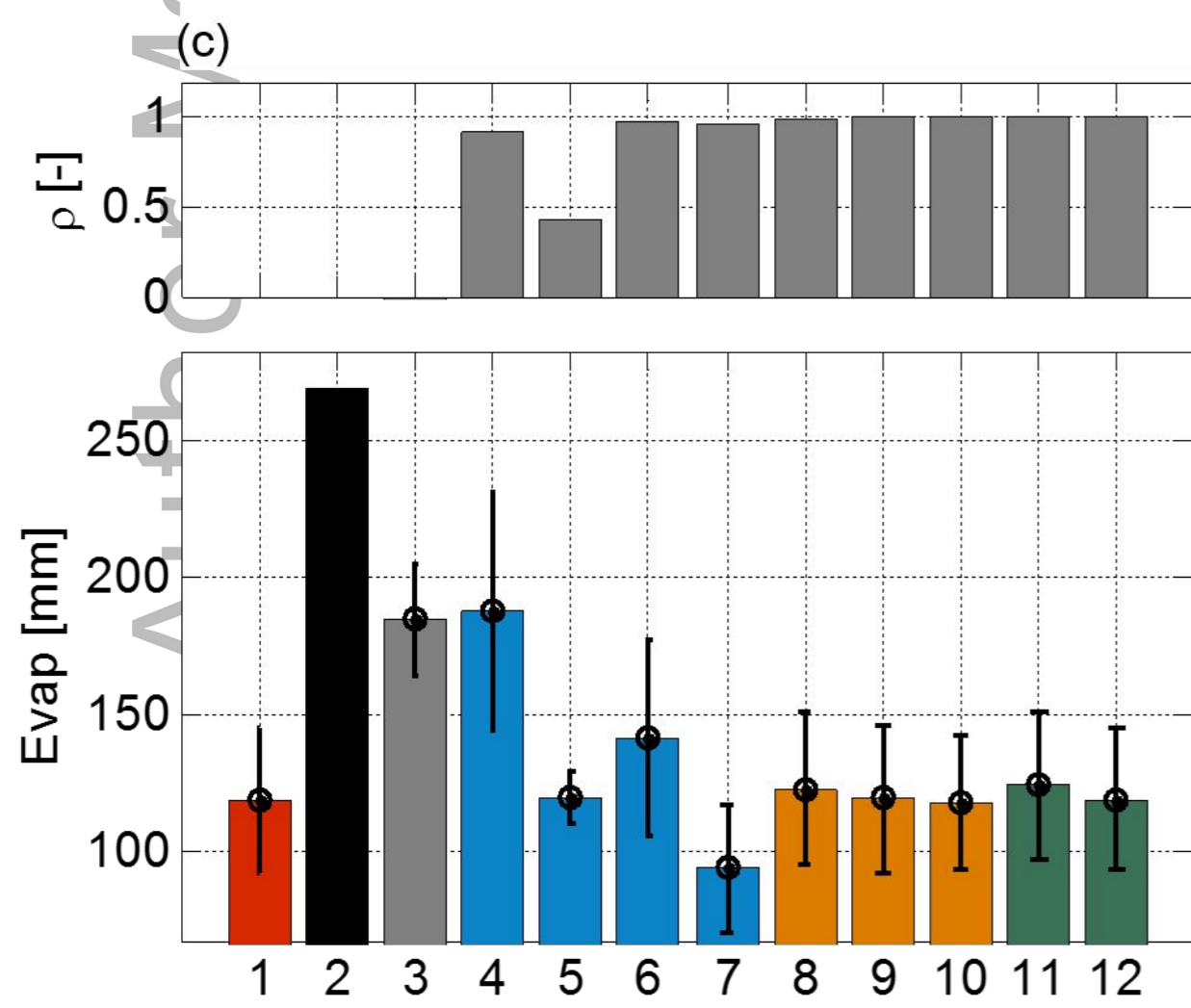
Figure 10: A schematic representation of the physical mechanisms explaining the effect of high frequency hydrometeorological variability on water/carbon fluxes, and transfer of variability across temporal scales.

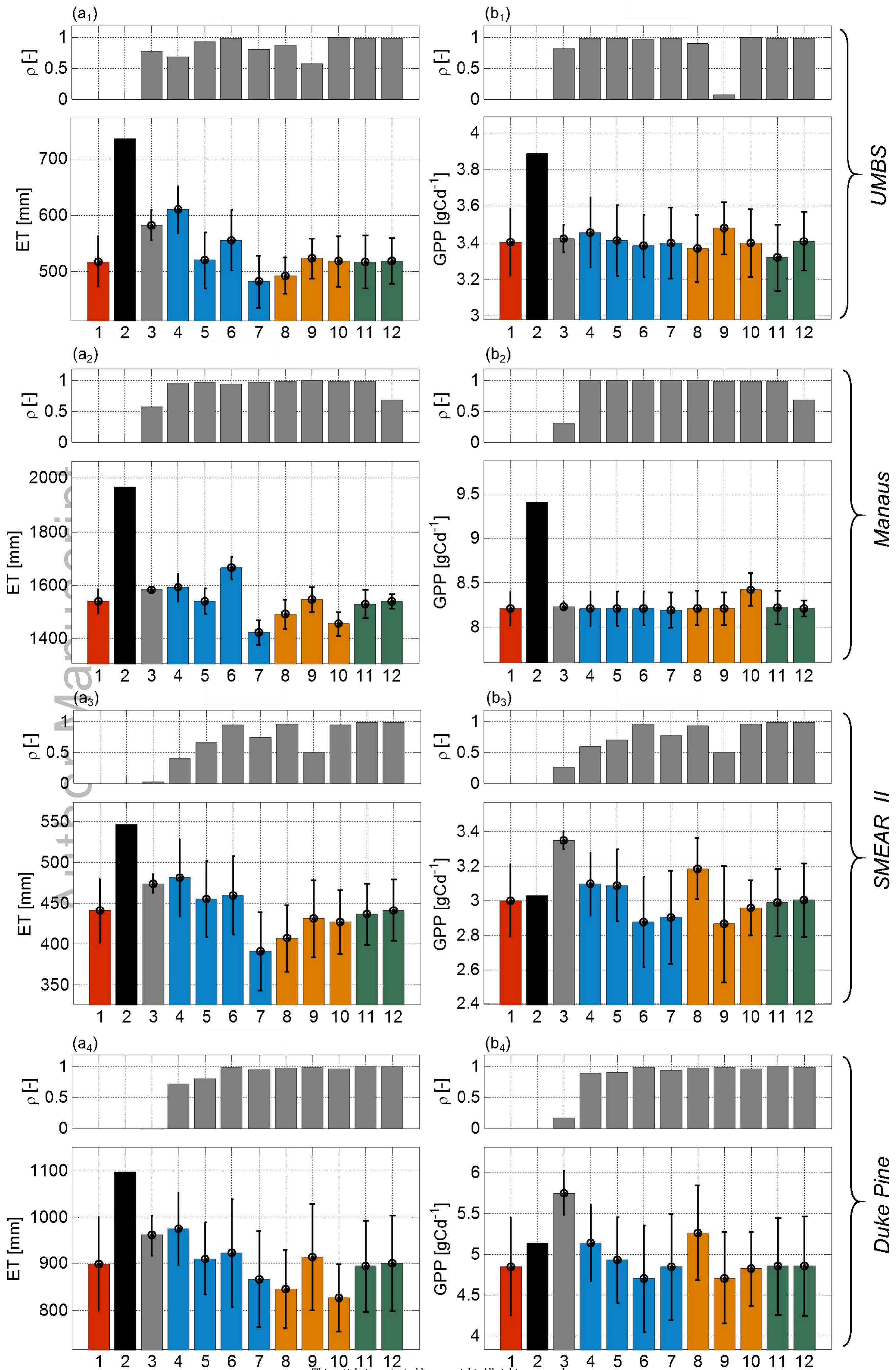


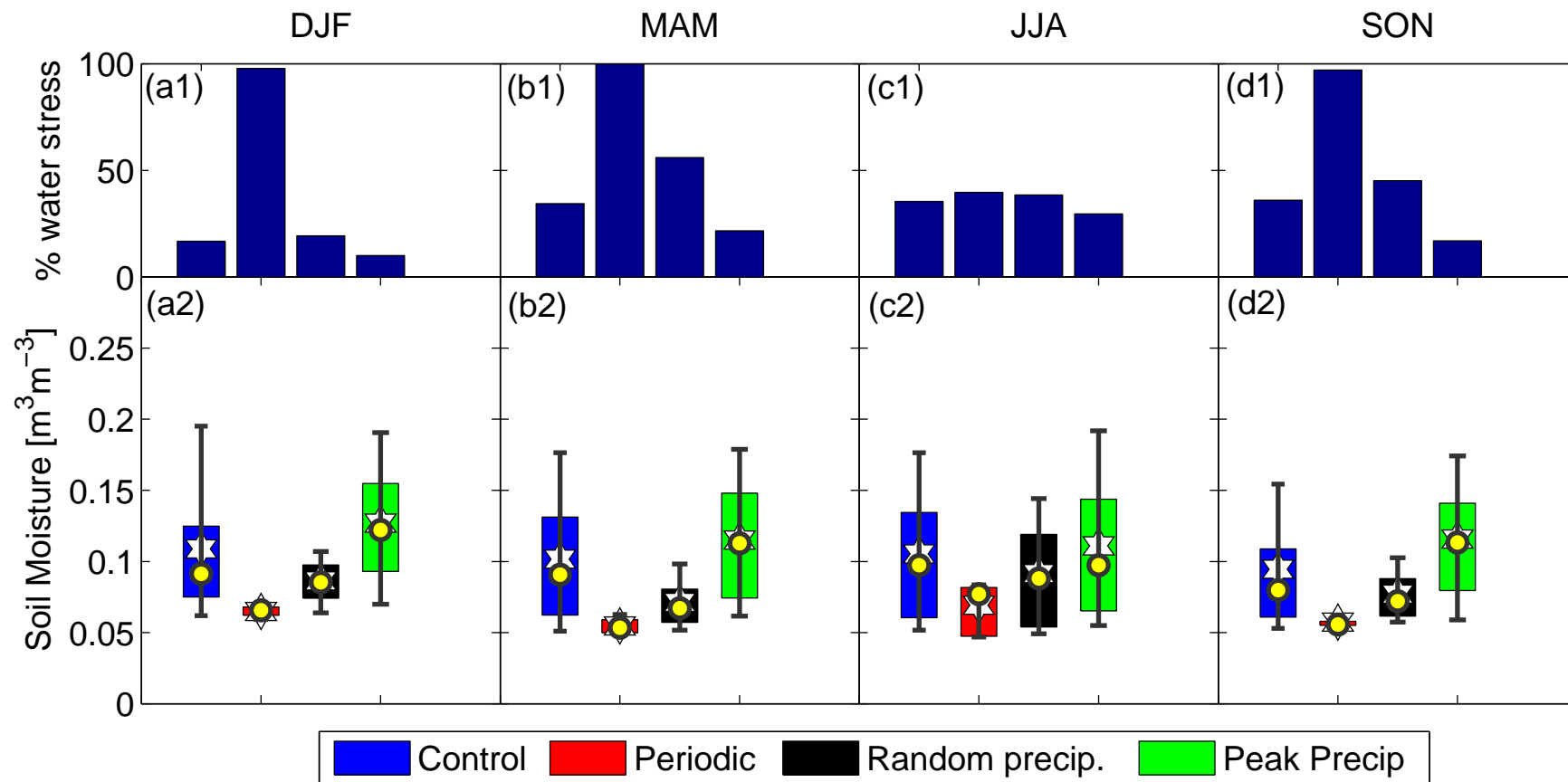




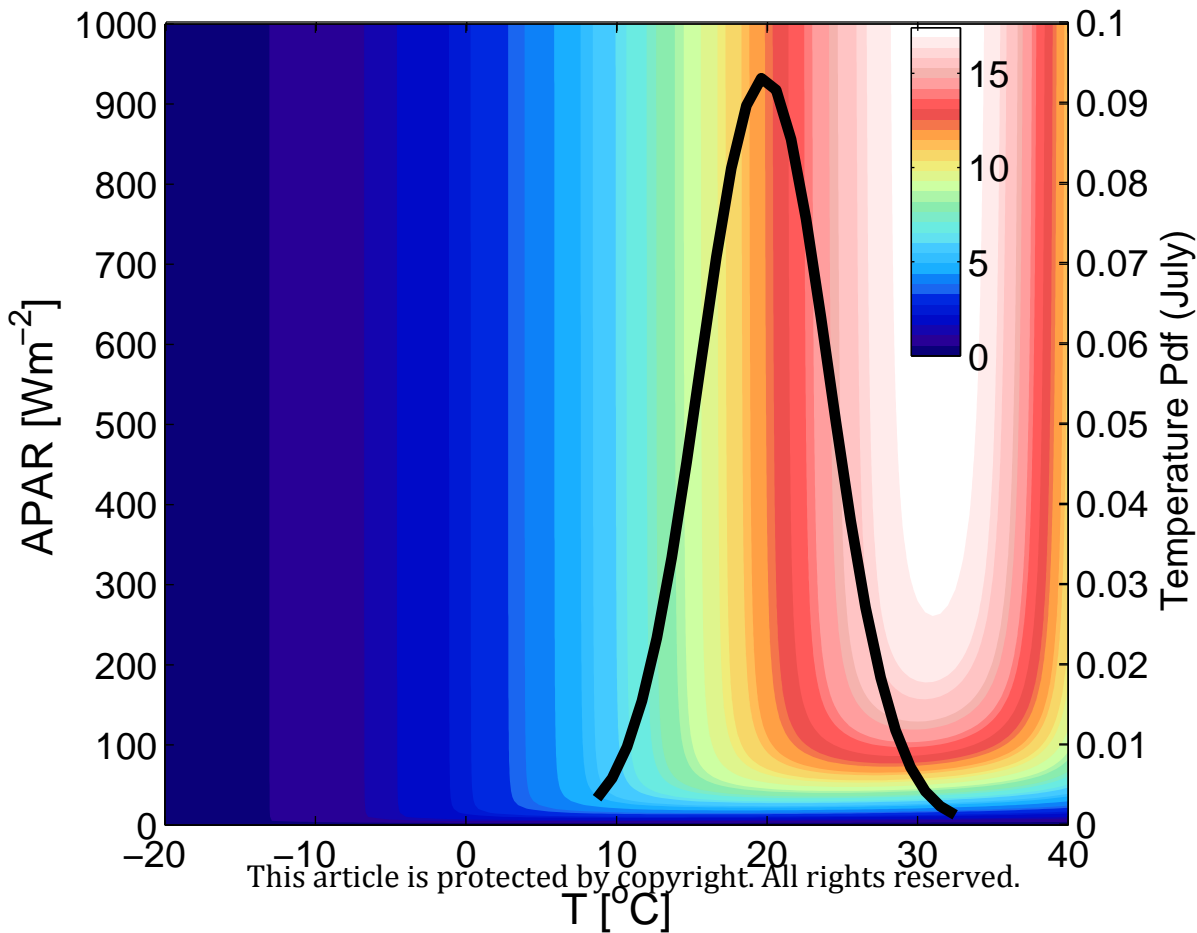
- 1: Original Input
- 2: Periodic Input
- 3: Randomized all input variables
- 4: Randomized Precip.
- 5: No IAV of Precip.
- 6: More Extreme Precip.
- 7: Less Extreme Precip.
- 8: Randomized Temperature
- 9: No IAV of Temperature
- 10: Smoothed Temperature
- 11: Randomized Radiation
- 12: No IAV of Radiation



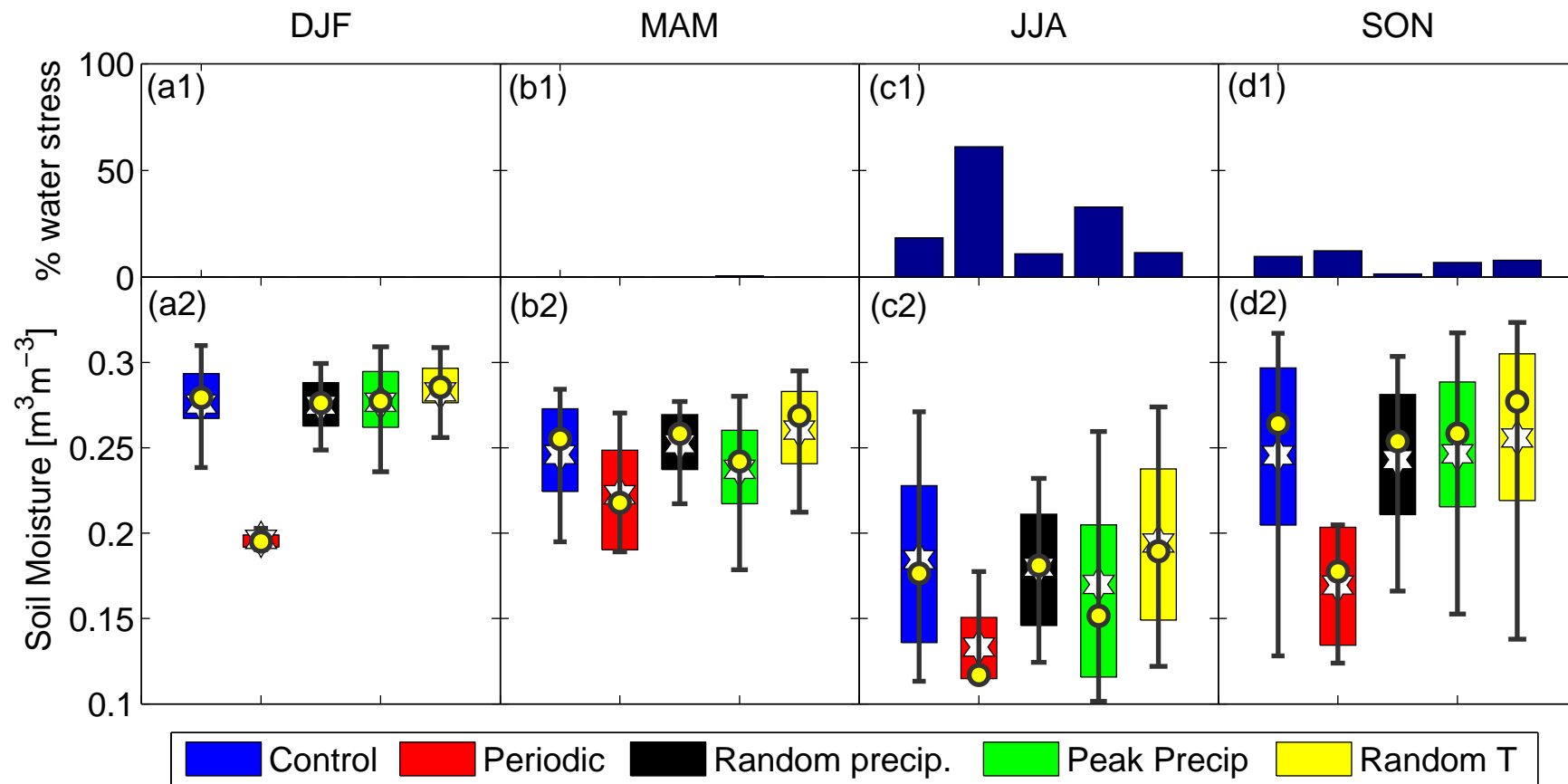


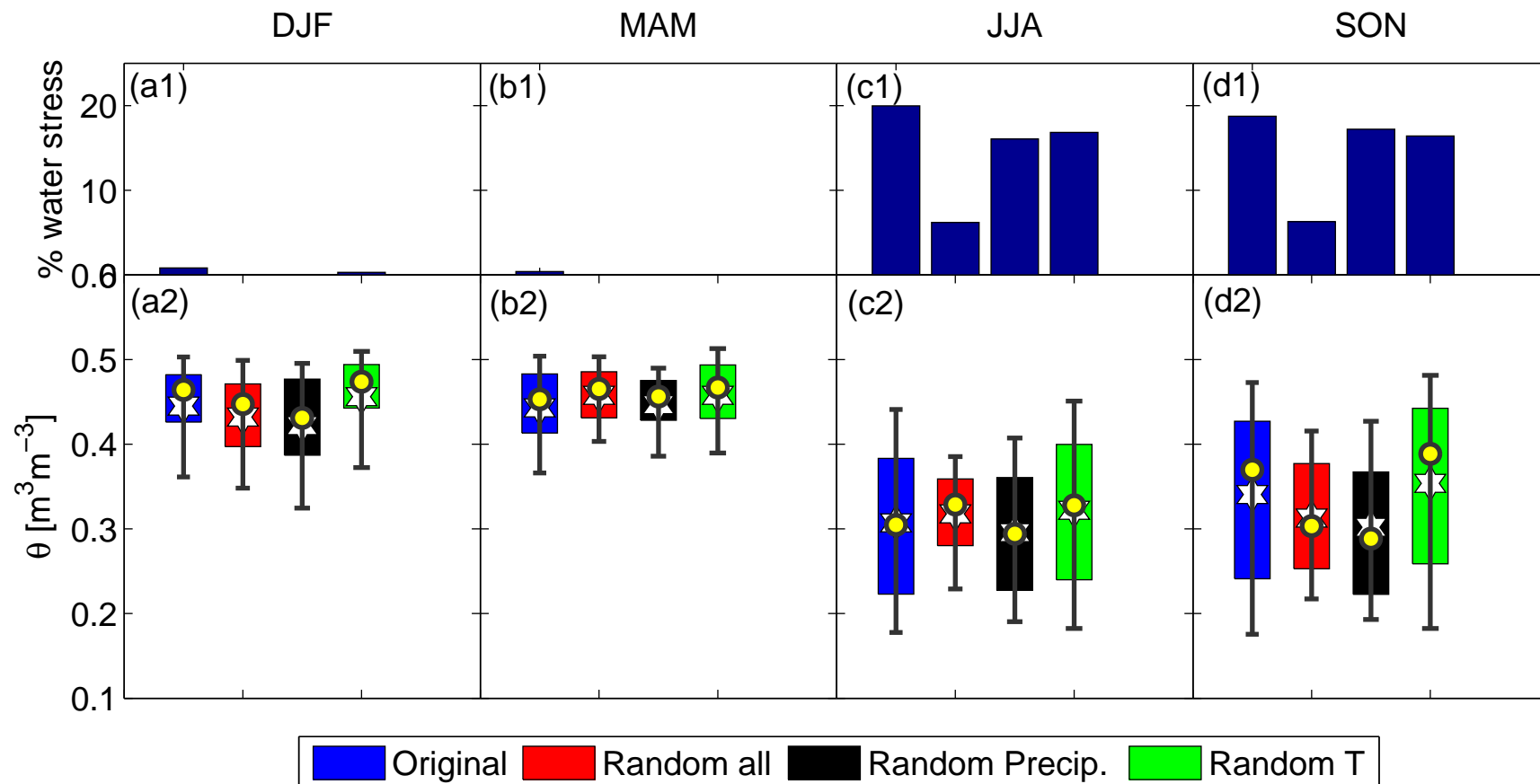


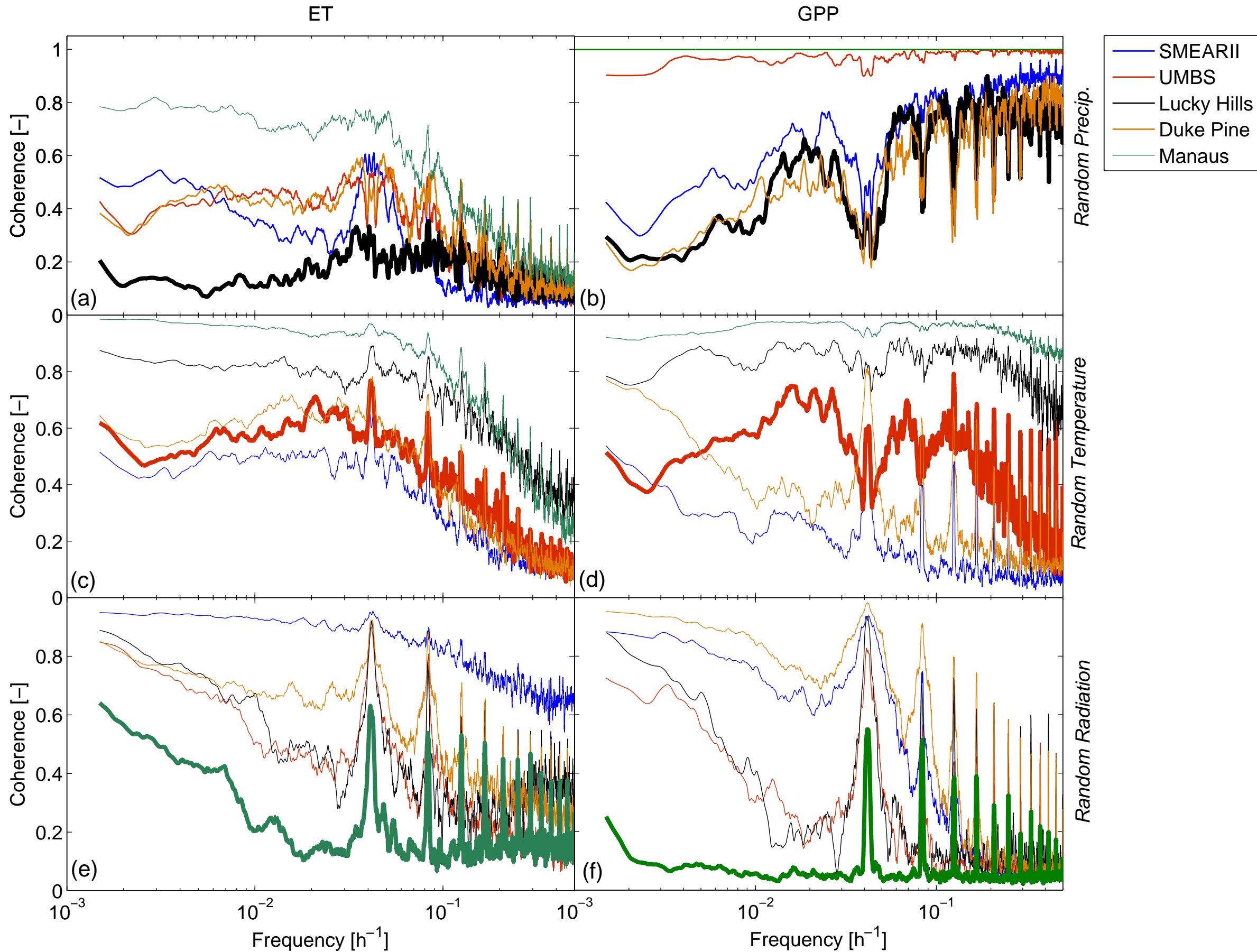
Gross Photosynthesis [$\mu\text{molCO}_2\text{m}^{-2}\text{s}^{-1}$]



This article is protected by copyright. All rights reserved.







Effects of high frequency hydrometeorological variability on water/carbon fluxes

(A) Precipitation variability:

- Water Interception/throughfall
 - Water in the interception storage
- Infiltration**
- Partition of runoff and infiltration
 - Soil water content in shallow soil layers
- Water percolation**
- Soil water content in deep soil layers

(B) Temperature variability:

- Energy balance**
- Leaf temperature + soil water content
- Biochemistry of photosynthesis**
- Non linear response of carbon assimilation to temperature

(C) Radiation variability:

- Energy balance**
- Leaf temperature + soil water content
- Biochemistry of photosynthesis**
- Non linear response of carbon assimilation to PAR

Effects on Photosynthesis and Transpiration

- Direct impact of (B) and (C) to the biochemistry of photosynthesis
- Indirect effect of (A) due to soil water availability, and (B), (C) by altering the energy balance also affects soil water availability

Effects on Soil Water Storage

- Direct impact of (A)
- Indirect effect of (B) and (C) by altering the energy balance

